

338

A STUDY OF THE EFFECT OF BAR
CUT-OFF ON THE SHEAR STRENGTH
OF RESTRAINED REINFORCED
CONCRETE BEAMS

SEPTEMBER 1966

NO. 18

Joint
Highway
Research
Project

by

G. R. SPAMAN

PURDUE UNIVERSITY
LAFAYETTE INDIANA

Final Report

A STUDY OF THE EFFECT OF BAR CUT-OFF
ON THE SHEAR STRENGTH OF RESTRAINED REINFORCED
CONCRETE BEAMS

TO: Dr. G. A. Leonards, Director
Joint Highway Research Project

September 20, 1956

FROM: H. L. Michael, Associate Director
Joint Highway Research Project

File: 7-4-10
Project: C-36-56J

The attached Final Report entitled "A Study of the Effect of Bar Cut-Off on the Shear Strength of Restrained Reinforced Concrete Beams" has been prepared by Mr. G. R. Spenn, Graduate Assistant on our staff. Professor M. J. Gutzwiller provided direction of the research.

The research reported was a continuation of research initiated and previously reported to this Board by W. H. Harvey. That research found that the use of current AASHO specifications with respect to allowing longitudinal bars to be cut off in the tension zone might not provide desirable safety. The research reported herein further investigated this problem.

The report is presented to the Board for the record.

Respectfully submitted,

H. L. Michael

H. L. Michael
Associate Director

HLM:ar

Attachments

Copy: F. L. Ashbaucher
J. R. Cooper
J. W. Delleur
W. L. Dolch
W. E. Goez
W. L. Grecco
G. K. Hallock
F. S. Hill
J. P. McLaughlin

F. B. Mendenhall
R. D. Miles
J. C. Oppenlander
W. P. Privette
M. B. Scott
F. W. Stubbs
K. B. Woods
E. J. Yoder

Final Report

A STUDY OF THE EFFECT OF BAR CUT-OFF
ON THE SHEAR STRENGTH OF RESTRAINED REINFORCED
CONCRETE BEAMS

by

G. R. Sparan

Graduate Assistant

Joint Highway Research Project

Project No: C-36-56J

File No: 7-4-10

Purdue University

Lafayette, Indiana

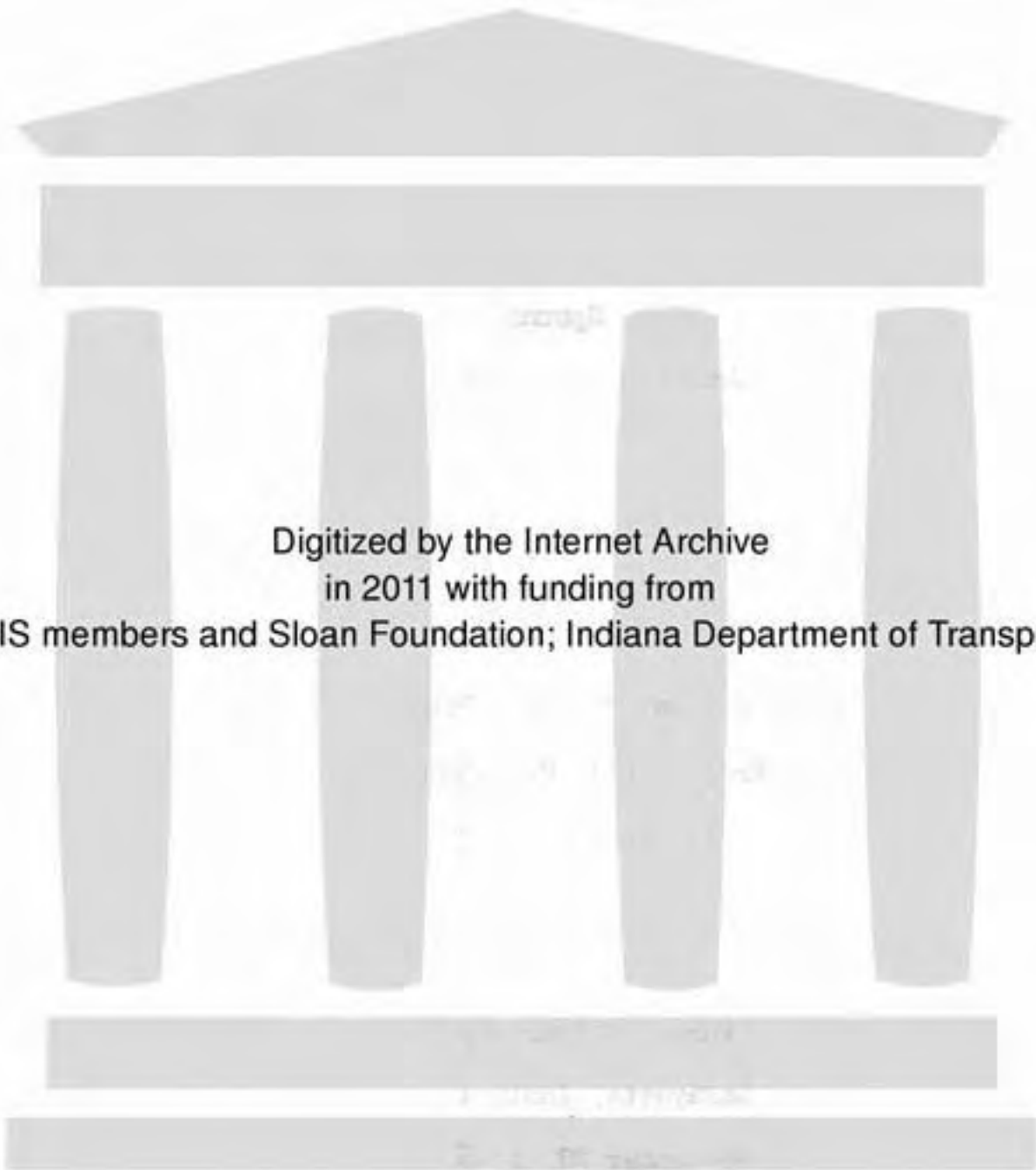
September 22, 1966

Digitized by Google

A STUDY OF THE EFFECT OF THE

CONSTRUCTION OF THE NEW YORK STATE

THRUWAY



Digitized by the Internet Archive
in 2011 with funding from

LYRASIS members and Sloan Foundation; Indiana Department of Transportation

LIST OF FIGURES

Figure	Page
1. Details of Specimens	4
2. Concrete Strain Distribution-Beam IA	11
3. Concrete Strain Distribution-Beam IB	12
4. Concrete Strain Distribution-Beam IC	13
5. Concrete Strain Distribution-Beam ID	14
6. Concrete Strain Distribution-Beam IE	15
7. Steel Strain vs. Gage Location-Beams IA and IB	16
8. Steel Strain vs. Gage Location-Beams IC and ID	17
9. Load vs. Deflection-Series I	18
10. Beam IA	19
11. Beam IB	20
12. Beam IC	21
13. Beam ID	22
14. Beam IE	23
15. Concrete Strain Distribution-Beam IIA	26
16. Concrete Strain Distribution-Beams IIB and IID	27
17. Concrete Strain Distribution-Beam IIC	28
18. Steel Strain vs. Gage Location-Beams IIA and IIC	29
19. Load vs. Deflection-Series II	30
20. Beam IIA	31
21. Beam IIB	32
22. Beam IIC	33
23. Beam IID	34
24. Concrete Strain Distribution-Beam IIIC	36

LIST OF FIGURES (CONTINUED)

Figure	Page
25. Steel Strain vs. Gage Location-Beam IIIC	37
26. Load vs. Deflection-Series III	38
27. Beam IIIB	39
28. Beam IIIC	40
29. Beam IIID	41
30. Comparison of AASHTO and ACI Allowable Shear Strengths for Beams Without Web Reinforcement	44
31. Formation of Diagonal Tension Crack	46
32. Development of Unsymmetrical Bending	48

LIST OF TABLES

Table	Page
1. Beam Designations	5
2. Properties of Beam Specimens	6
3. Summary of Test Results	8
4. Comparison of Test Strengths with ACI-ASCE Committee 326 Recommendations	50
5. Comparison of Test Strengths with AASHTO "Standard Specifications for Highway Bridges"	53

INTRODUCTION

The Problem

The problem was defined in a prior Joint Highway Research Project Report by W. N. Harvey (4)*. Harvey found that a definite lack of safety existed in the present AASHO "Standard Specifications for Highway Bridges" (3) with respect to allowing longitudinal bars to be cut off in the tension zone. Beams having the AASHO cut-off point were found to have a reduction in both the diagonal cracking load and the ultimate shear strength.

For a more extensive development of diagonal tension failure and shear strength, the reader is referred to Harvey's report.

Purpose and Scope

The objective of this study was to observe the behavior of beams having different cut-off points for the longitudinal tension reinforcement. In addition, the effects of web reinforcement and concrete strength on the beams were also observed.

The tests were limited to beams of rectangular cross section and one set of loading conditions. An attempt was made to correlate the effect of the formation of the diagonal tension crack upon the distribution of steel strain along the remaining negative reinforcing bar and upon the possible unsymmetrical bending due to the cut-off bar.

* Numbers in parenthesis refer to BIBLIOGRAPHY at end of report.

TEST SPECIMENS AND PROCEDURES

The physical properties of the test beams and the testing procedure conformed to the procedure for Series II beams as outlined in Harvey's report with only a few exceptions.

First, the major variable in this report was the location of the tension reinforcement cut-off point. The allowable cut-off point according to the AASHTO Specifications (3) is "at least 15 diameters but not less than 1/20 of the span length beyond the point at which computations indicate it is no longer needed to resist stress." In contrast, the ACI Specifications (2) provide for three alternatives:

"918...

- (b) Except at supports, every reinforcing bar shall be extended beyond the point at which it is no longer needed to resist flexural stress, for a distance equal to the effective depth of the member or 12 bar diameters, whichever is greater.
- (c) No flexural bar shall be terminated in a tension zone unless one of the following conditions is satisfied:
 1. The shear is not over half that normally permitted, including allowance for shear reinforcement, if any.
 2. Stirrups in excess of those normally required are provided each way from the cut off a distance equal to three-fourths of the depth of the beam. The excess stirrups shall be at least the minimum specified in Section 1206(b) or 1706(b). The stirrup spacing shall not exceed $d/8r_b$ where r_b is the ratio of the area of bars cut off to the total area of bars at the section.

3. The continuing bars provide double the area required for flexure at that point or double the perimeter required for flexural bond."

Hence, in the test program undertaken, test specimens were prepared having the cut-off at (1) the theoretical cut-off point, (2) the AASHTO cut-off point, (3) the ACI alternate 2), and (4) the ACI alternate 3). In addition, the specimens were placed into two groups - with and without web reinforcement. Figure 1 gives the applied shears, moments and the locations of bar cut-off. Note that due to the particular physical properties of the test beams the cut-off for ACI alternate 2) and the AASHTO cut-off coincide. Hence, this beam was also used to determine the effectiveness of placing stirrups around the AASHTO cut-off point.

The other exceptions to the procedure outlined in Harvey's report were:

- 1) The continuing longitudinal bar had Budd Metalfilm strain gages placed upon it at the quarter points of the shear span (Figure 1). By using epoxy waterproofing compound and the metalfilm gages, bond was destroyed only over an area approximately 1/2" by 1" per gage.
- 2) A series using the AASHTO Specifications without web reinforcement was tested using concrete strength as a variable.
- 3) The surface concrete strains were measured using SR-4 strain gage lengths of 2 1/2" and 4". The gages were placed on each side of the beam 3 1/2" from the negative moment support and at 1", 2", and 3" up from the bottom face.

Tables 1 and 2 give the beam designations and the physical properties of the beams. As noted in Table 1, some of the test results of Harvey's report were used per se in this report in order to provide a more comprehensive study and also to eliminate unnecessary duplication.

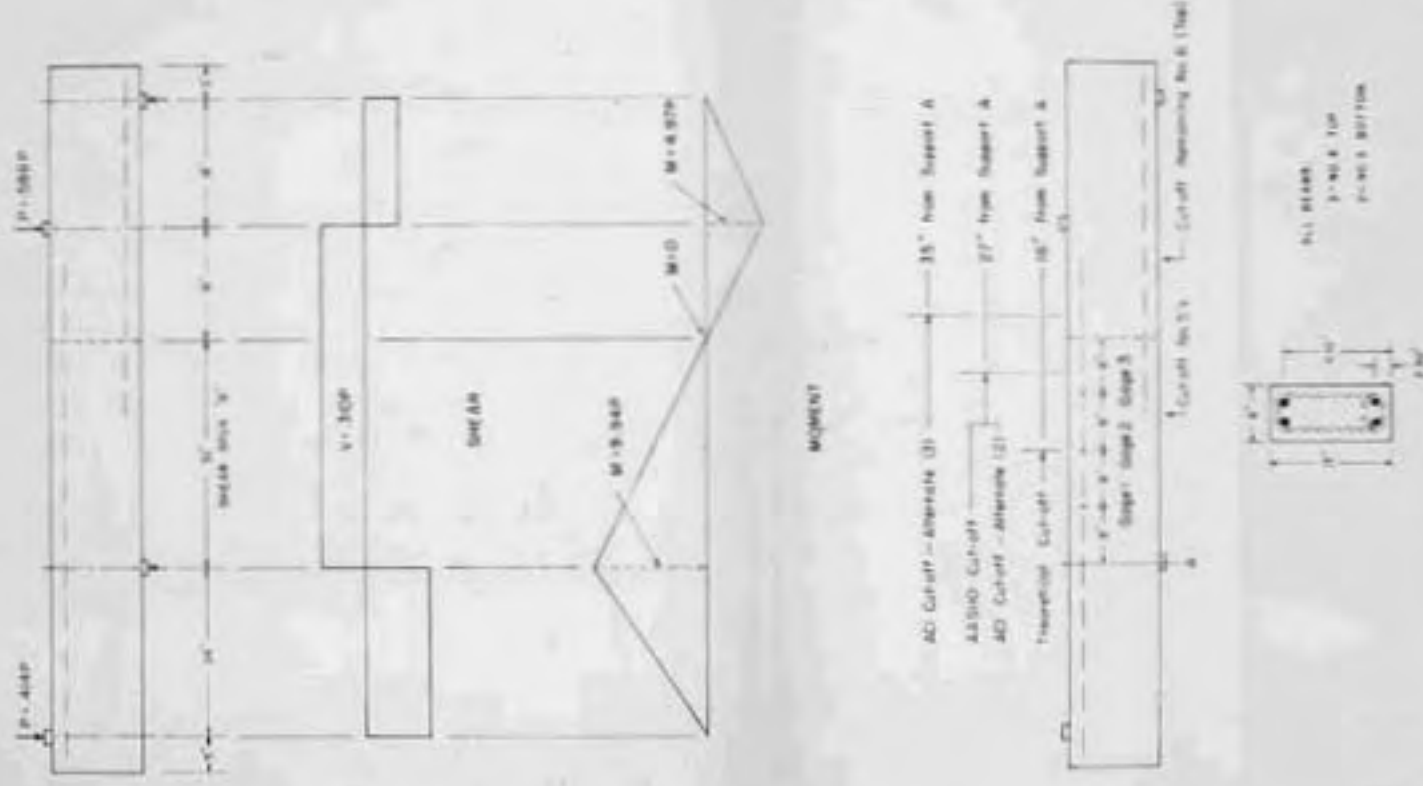


FIGURE 1. DETAILS OF SPECIMENS

LOCATION OF BAR CUT-OFF AND BEAM CROSS SECTION

TABLE 1.

BEAM DESIGNATIONSSERIES I Without Stirrups

- IA Theoretical Cut-off
- IB AASHO Cut-off
- IC ACI Cut-off - Alternate (3) (Double Area)
- ID ACI Cut-off - Alternate (2)
- IE No Cut-off*

SERIES II With Stirrups (No. 4 Wire at 3 1/2")

- IIA Theoretical Cut-off
- IIB AASHO Cut-off*
- IIC ACI Cut-off - Alternate (3) (Double Area)
- IID No Cut-off*

SERIES III AASHO Cut-off Without Stirrups -

Variable Concrete Compressive Strength

- IIIA $f_c' = 4380$ psi (Beam IB)
- IIIB $f_c' = 4360$ psi*
- IIIC $f_c' = 3340$ psi
- IIID $f_c' = 3620$ psi

* Results obtained from Harvey's report

TABLE 2.

PROPERTIES OF BEAM SPECIMENS

Beam Design- ation	Concrete Compressive Strength, f_c' psi	Concrete Split Tensile Strength f_c' (psi)	Initial Tangent Modulus E_c (psi $\times 10^6$)	Cut-off
IA	3600	354	3.84	West
IB	4380	478	3.91	East
IC	4120	336	3.68	East
ID	4100	350	3.77	East
IE	4380	356	3.55	No
IIA	4090	450	3.63	West
IIB	4210	379	3.24	East
IIC	4520	436	3.82	East
IID	4590	477	3.94	No
IIIA (IB)	4380	478	3.91	East
IIIB	4360	416	4.06	West
IIIC	3340	290	3.84	West
IIID	3620	279	3.44	West

TEST RESULTS

Table 3 gives a tabular summary of the pertinent test results for all beams tested. Strain and deflection measurements for each beam are presented graphically in this section. In addition, a brief description of each test is given in an attempt to correlate the recorded measurements with the progression of cracks and with particular observations made during the tests.

All loads reported herein are the loads applied by the testing machine.

For beams without web reinforcement the load at formation of the diagonal tension crack was in most cases easily determined. The effects of the crack's penetration into the compression zone were generally immediate. However, for beams with web reinforcement the stress redistribution was gradual, and a definite diagonal cracking load was often difficult to determine. For this reason the diagonal cracking load is defined herein as the load at which the critical diagonal crack was observed to cross the theoretical cracked section neutral axis. The cracked section neutral axis for the beams of this investigation ranged from 4.0" to 4.2" from the compression face.

TABLE 3.

SUMMARY OF TEST RESULTS

Beam Designation	Diagonal Cracking Load	Ultimate Load	Shearing Stress at Diagonal Cracking	Ultimate Shearing Stress
	P_c^* (kips)	P_u^* (kips)	v_c^{**} (psi)	v_u^{**} (psi)
IA	15	21	70	98
IB	23	31	107	144
IC	34	37	158	172
ID	37.5	37.5	174	174
IE	34	48	158	223
IIA	20	42	93	195
IIB	35	59	163	274
IIC	35	58	163	269
IID	35	67	163	311
IIIA	23	31	107	144
IIIB	25	29.1	116	135
IIIC	29	29	135	135
IIID	32	32	149	149

* Total applied load (does not include dead weight of specimen and loading apparatus.)

** Average shearing stress, $v = \frac{V}{bd}$, in critical span

Series I

Beam IA

Flexural cracks began forming at 10^k (Figure 10) and Gage 1 indicated steel strain pick-up (Figure 7). At 15^k the critical diagonal tension crack was formed as an extension of a tension crack through the steel cut-off point and had propagated to the neutral axis on the west side. Definite signs of moment redistribution were indicated because the steel strain at Gage 2 was larger than the steel strain at Gage 1. By 18^k the diagonal tension crack was within 1 1/2" of the compression face and the steel strain at Gage 2 was almost double that at Gage 1. The concrete strains still remained very low. The difference in crack progression on the two sides of the beam indicated that some unsymmetrical bending was occurring due to the steel cut-off. Finally, at 21^k the beam failed when the diagonal tension crack opened wide and the crack propagated along the continuing bar.

Beam IB

Flexural cracks had produced a strain take-up in Gage 1 by a load of 20^k . (Figures 7 and 11). The critical diagonal tension crack had already developed as an extension of a flexural crack on the east side of the beam midway between Gages 1 and 2 and had propagated to within an inch of the neutral axis. The diagonal tension crack crossed the neutral axis at 23^k . The steel strain at Gage 2 had almost overtaken the steel strain at Gage 1 at 27^k . The beam failed at 31^k as the diagonal tension crack propagated back to the longitudinal steel and then continued along it.

Beam IC

Flexural cracks had produced a take-up in the steel strains at 20^k (Figures 8 and 12). These progressed slowly until at 31^k the critical

diagonal tension crack began progressing toward the compression face as a continuation of a flexural crack. This crack had opened at 25^k at the location of Gage 2. At 34^k the crack crossed the neutral axis and the steel strain at Gage 2 began to overtake the steel strain at Gage 1. At 37^k the beam failed as the diagonal tension crack reached the compression face and also propagated along the entire length of the continuing longitudinal bar.

Beam ID

Flexural cracks had developed rather extensively by 30^k (Figures 8 and 13). However, the critical diagonal tension crack did not develop until the failure load of 37.5^k was reached. The crack angled from the compression face at 3" from the support up to the bar cut-off point and then along the continuing longitudinal bar. The steel strains remained in approximately the same proportions until failure, indicating no moment redistribution.

Beam IE

The vertical flexural tension crack (Figure 14), which eventually developed into the critical diagonal tension crack, started at about 12" from the support, bent to a 45° incline near middepth, and headed straight for the support. From 32^k to 34^k the diagonal crack penetrated into the compression zone to within 2" of the compressive face, extended back at 45° from middepth to the tension steel, and widened considerably.

Ultimate failure was by crushing of the concrete below the end of the diagonal crack at 48^k .

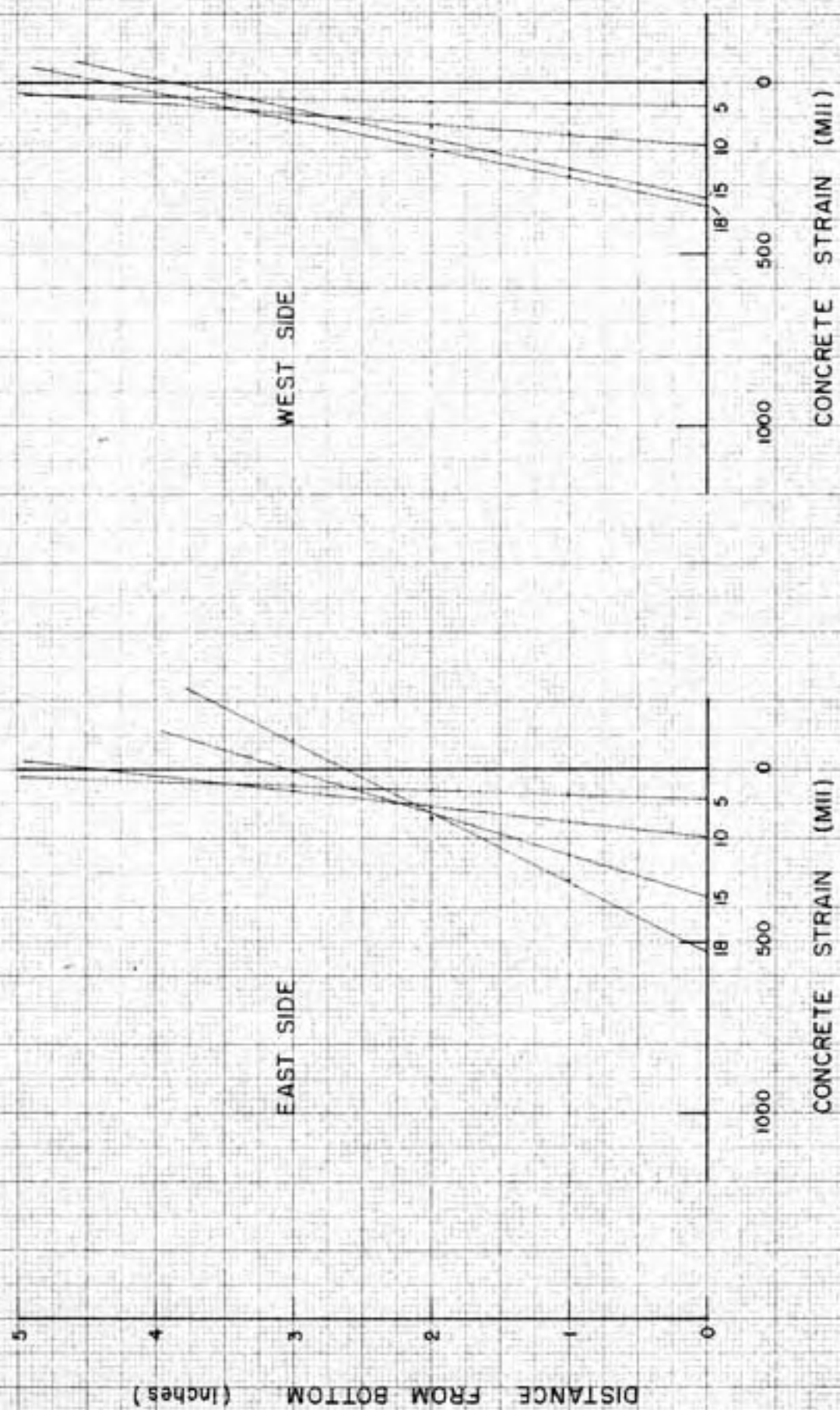


FIGURE 2. CONCRETE STRAIN DISTRIBUTION — BEAM 1A

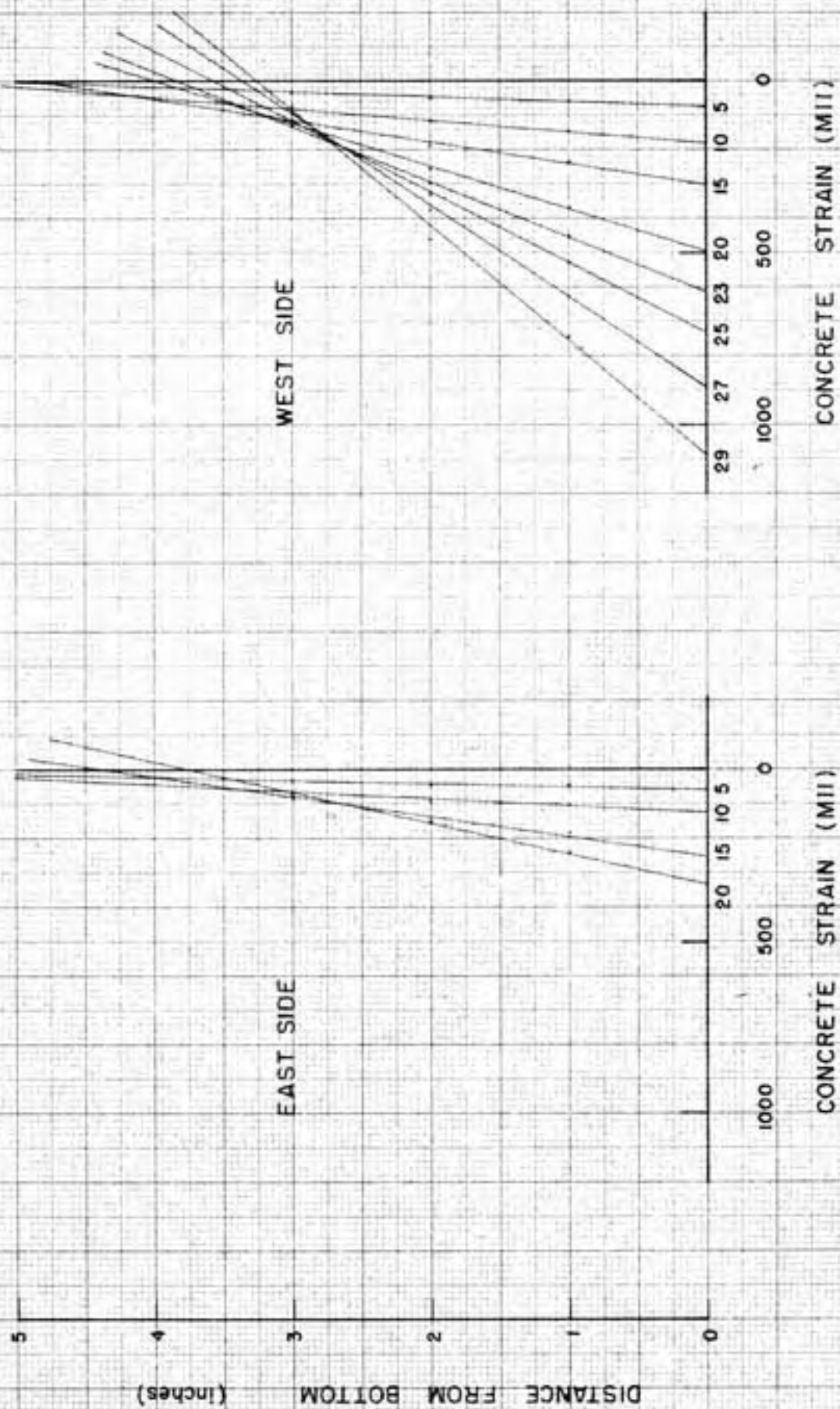


FIGURE 3. CONCRETE STRAIN DISTRIBUTION — BEAM IB

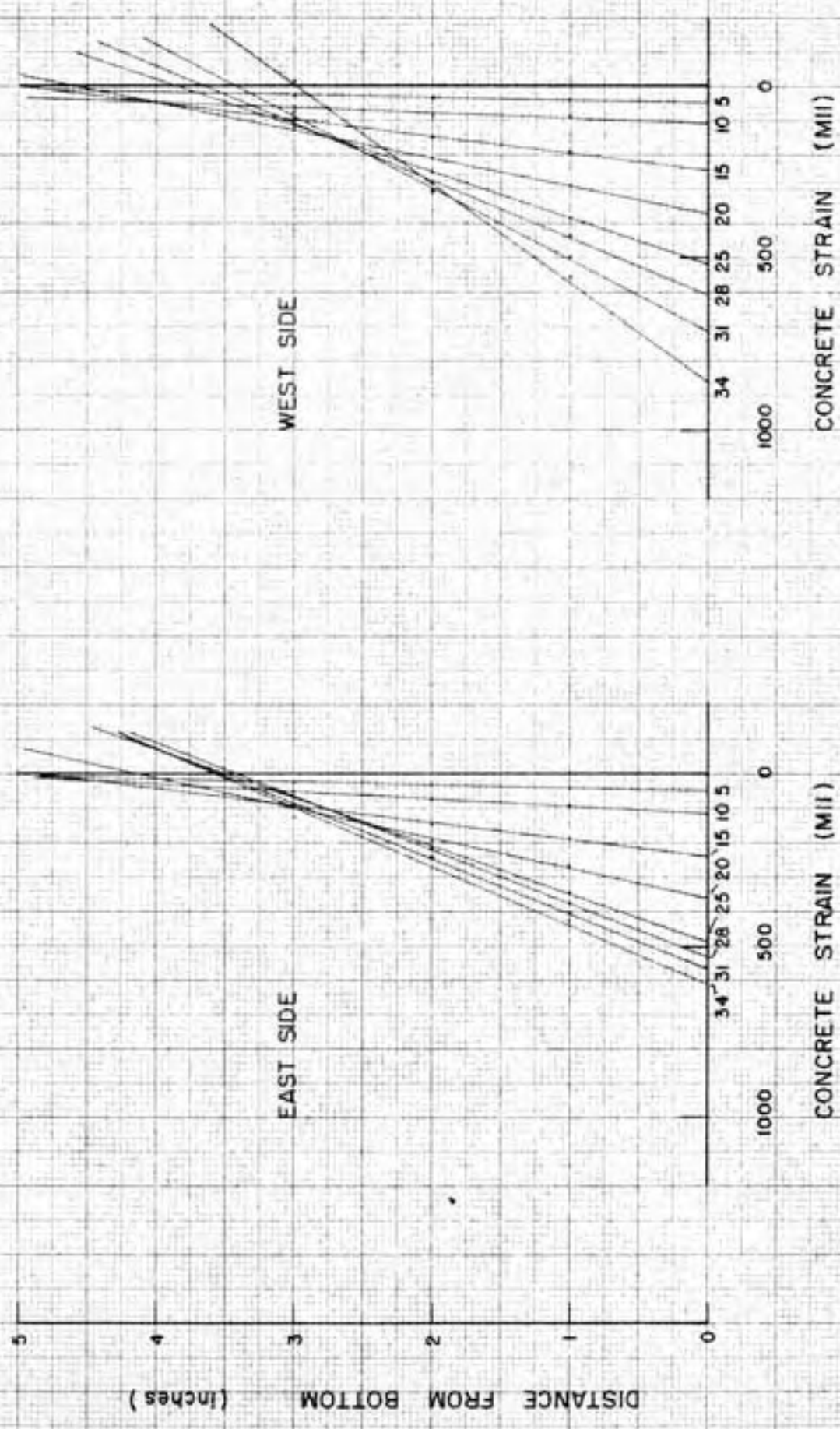


FIGURE 4. CONCRETE STRAIN DISTRIBUTION — BEAM IC

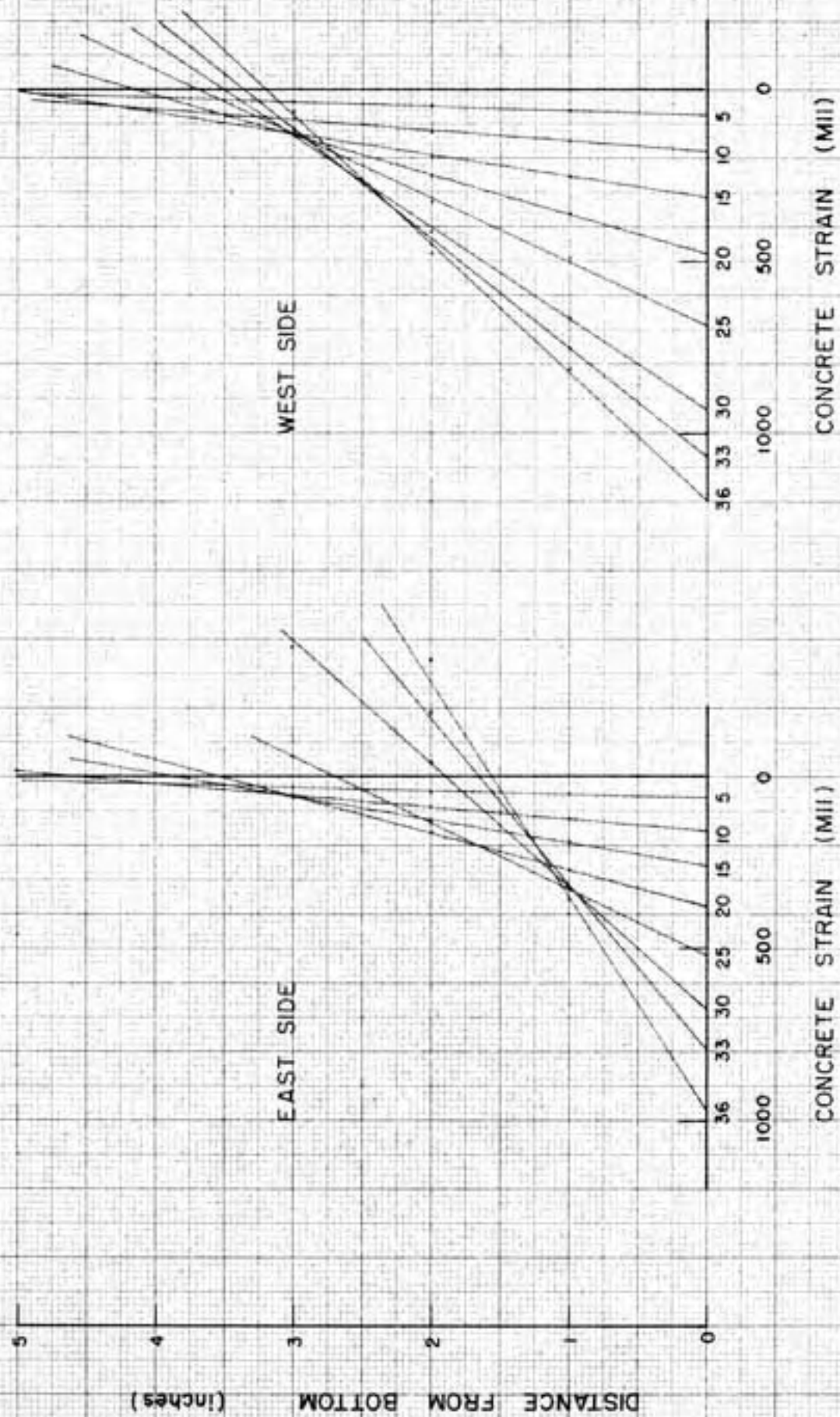


FIGURE 5. CONCRETE STRAIN DISTRIBUTION — BEAM ID

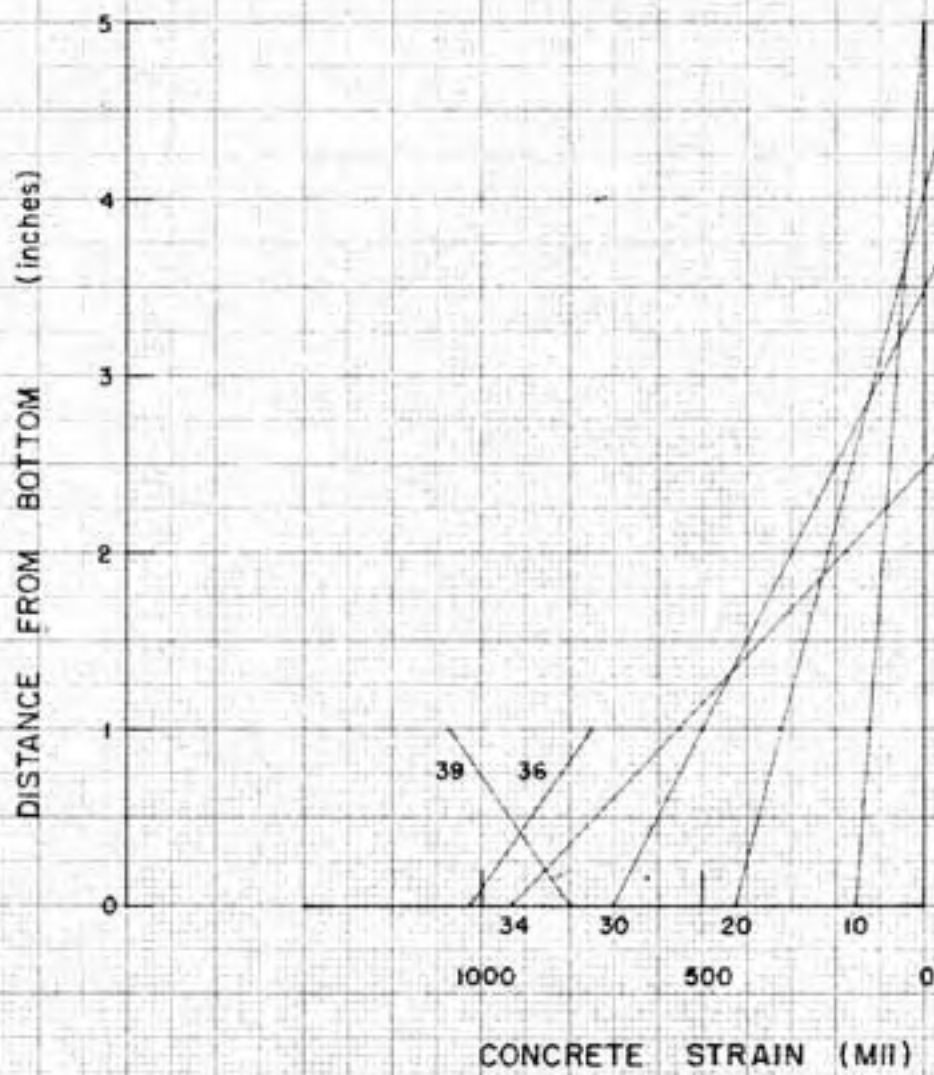


FIGURE 6. CONCRETE STRAIN DISTRIBUTION — BEAM IE

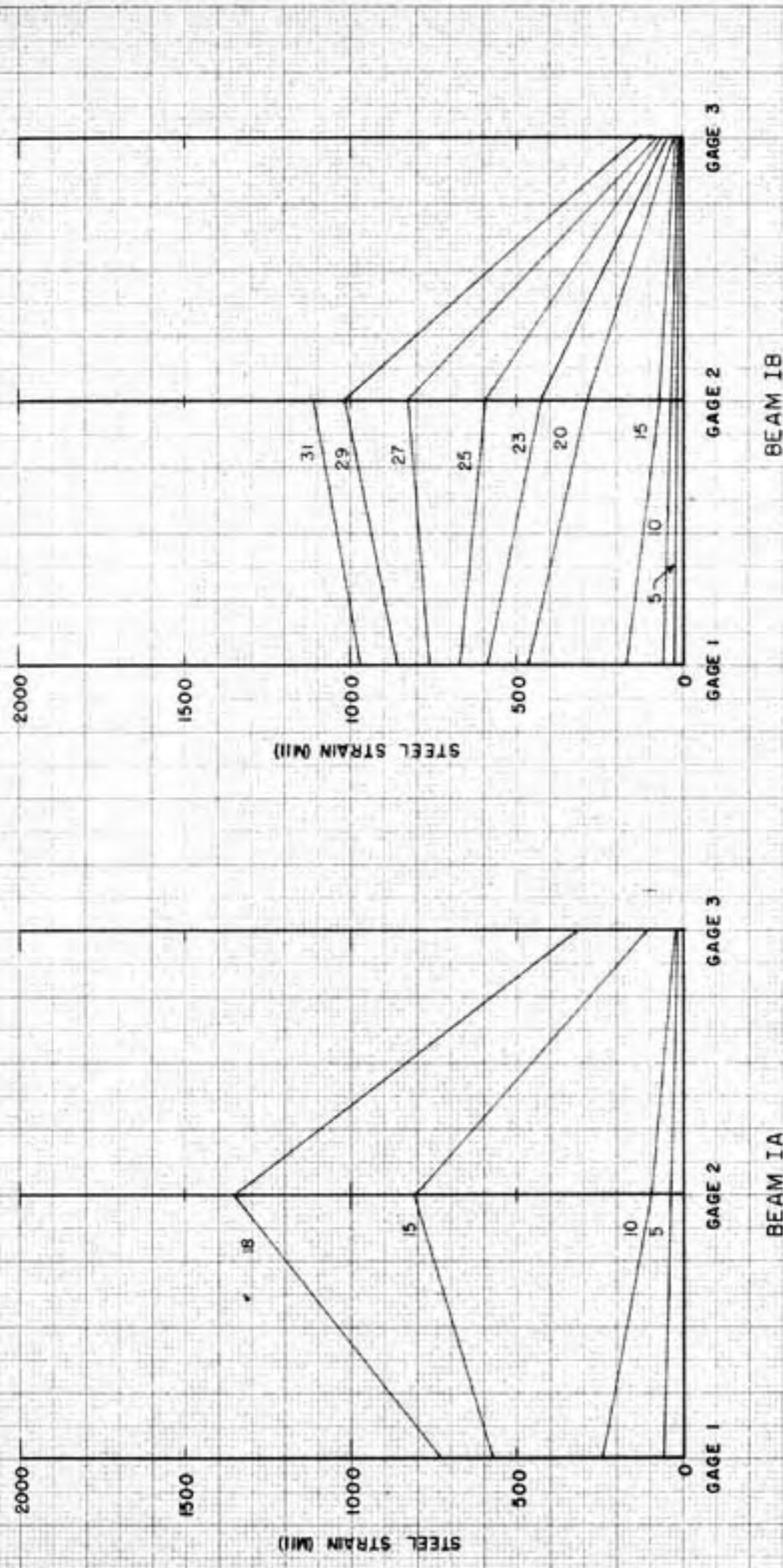


FIGURE 7. STEEL STRAIN vs. GAGE LOCATION — BEAMS IA and IB

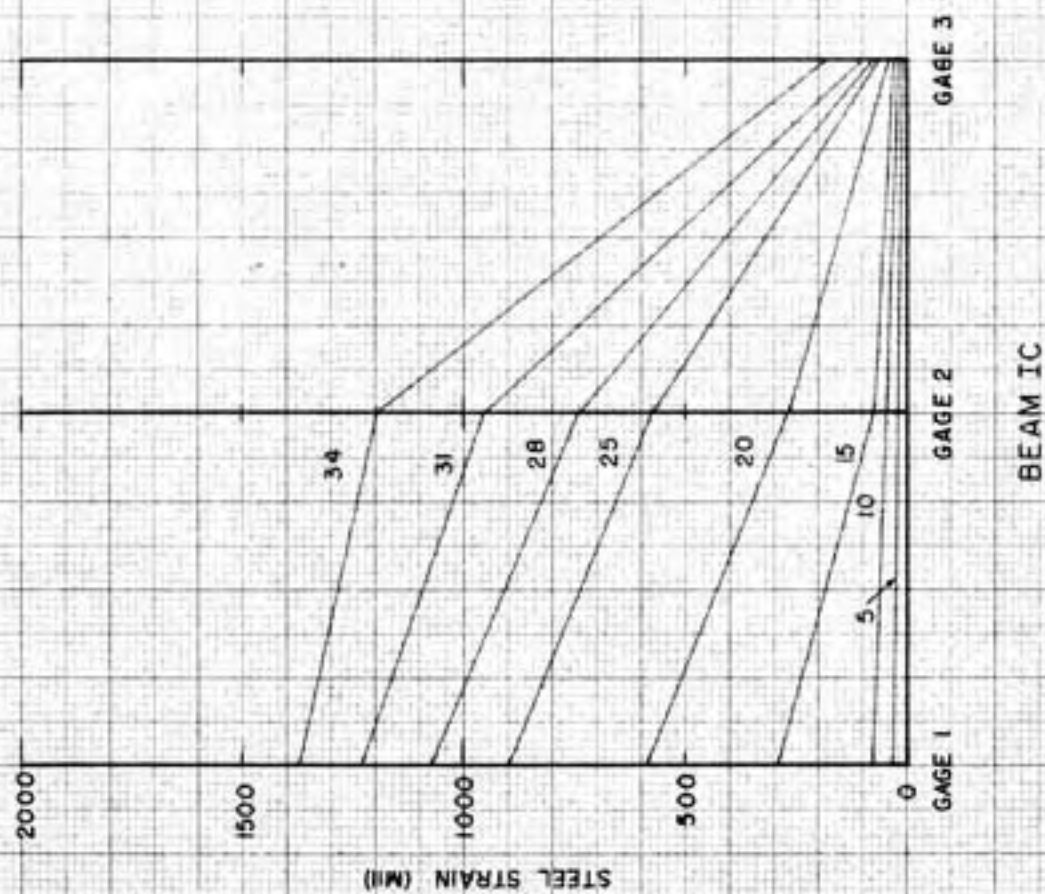
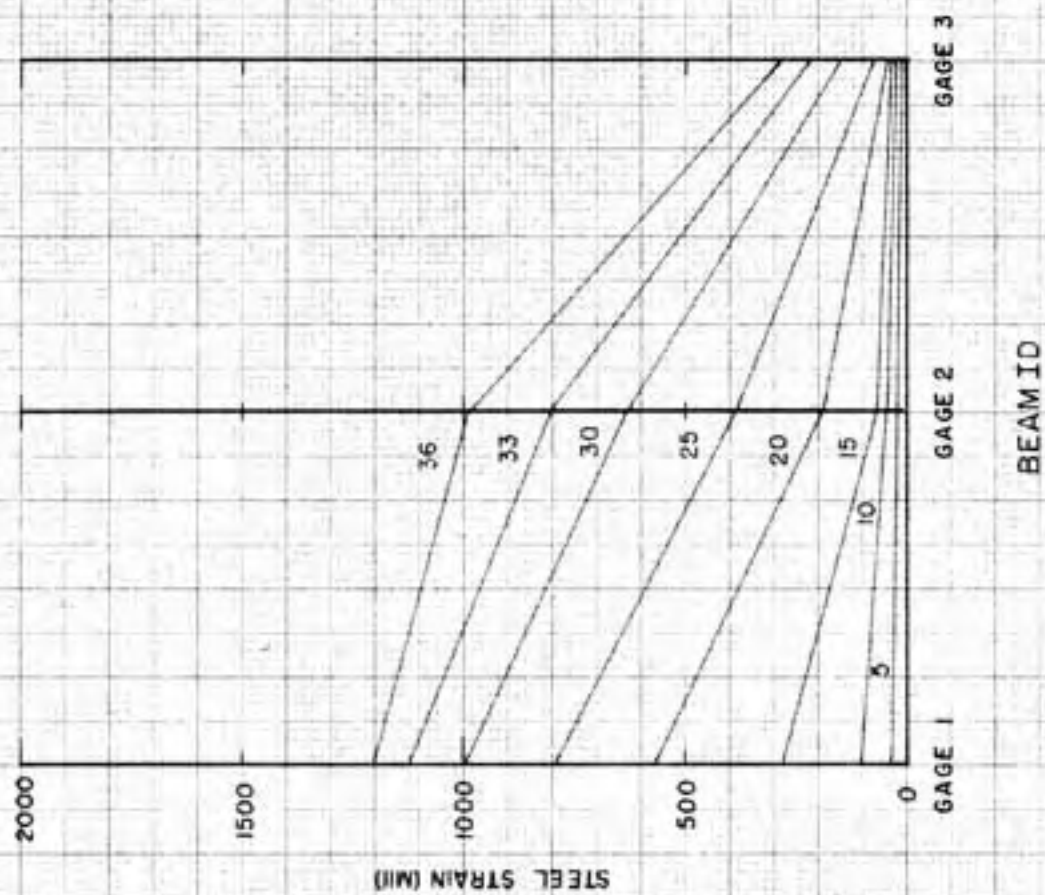


FIGURE 8. STEEL STRAIN vs. GAGE LOCATION — BEAMS IC and ID

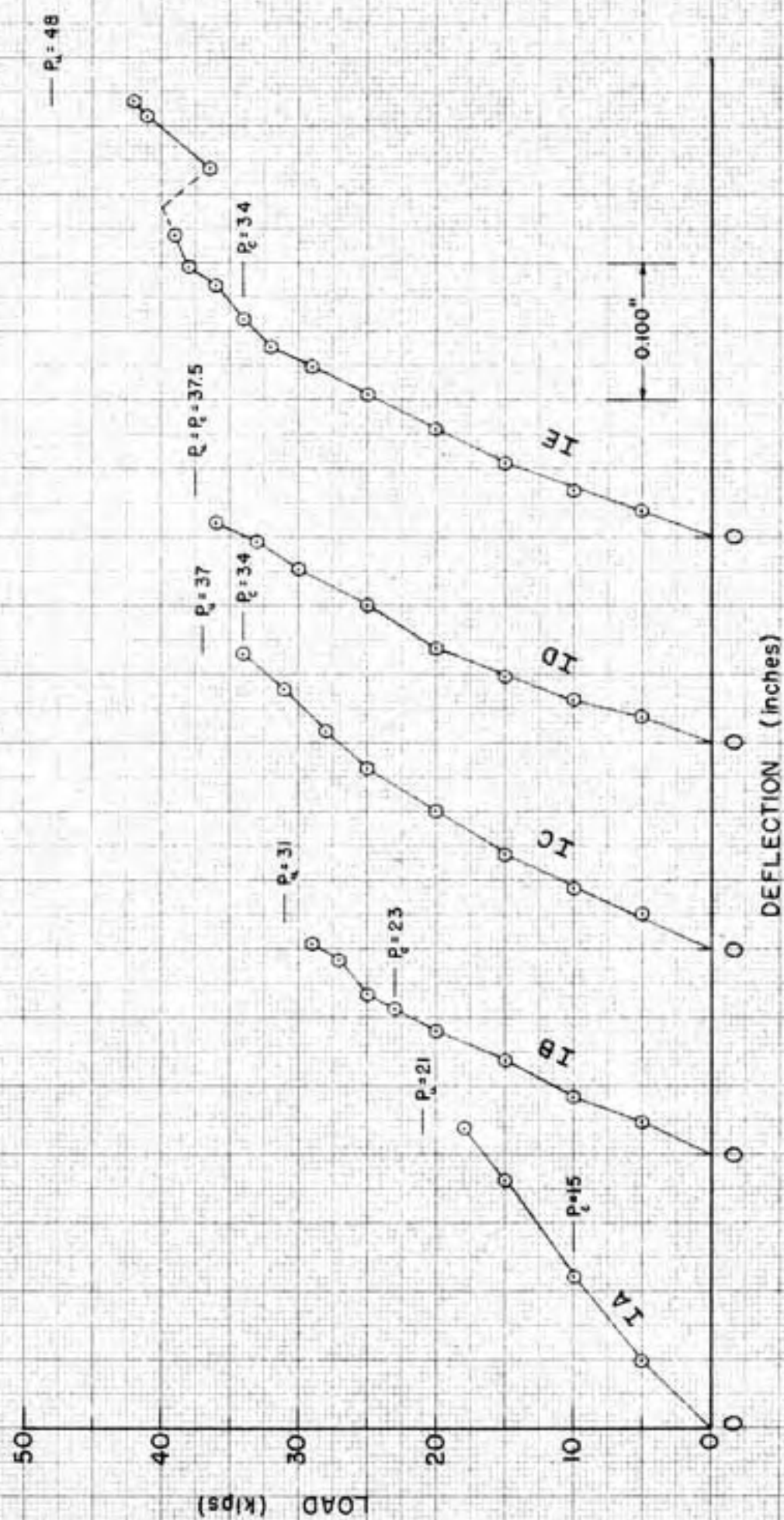
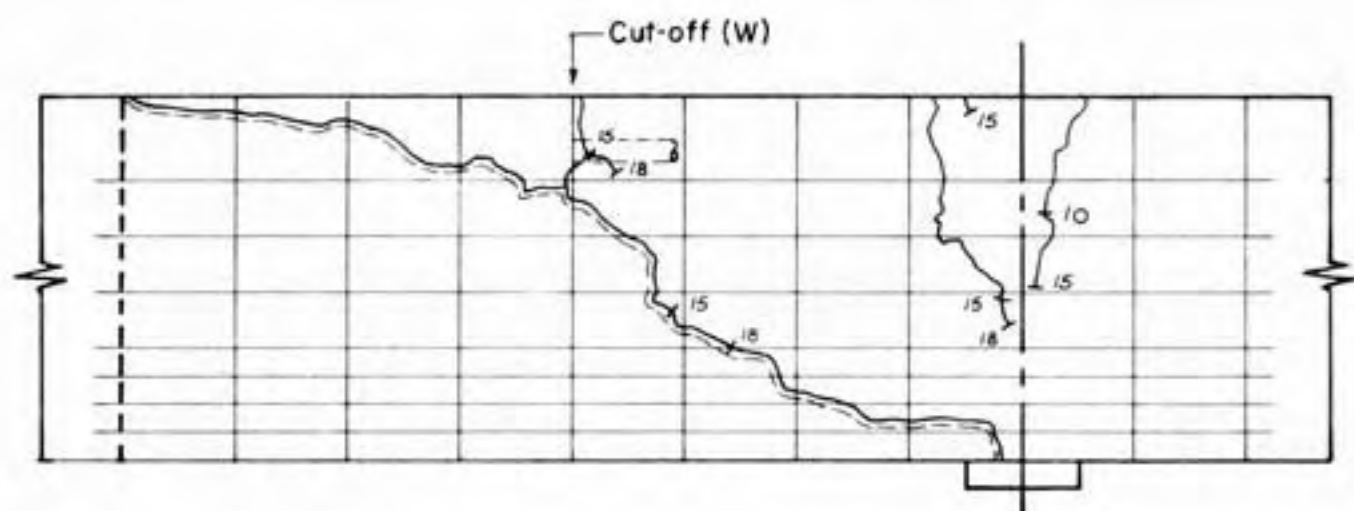
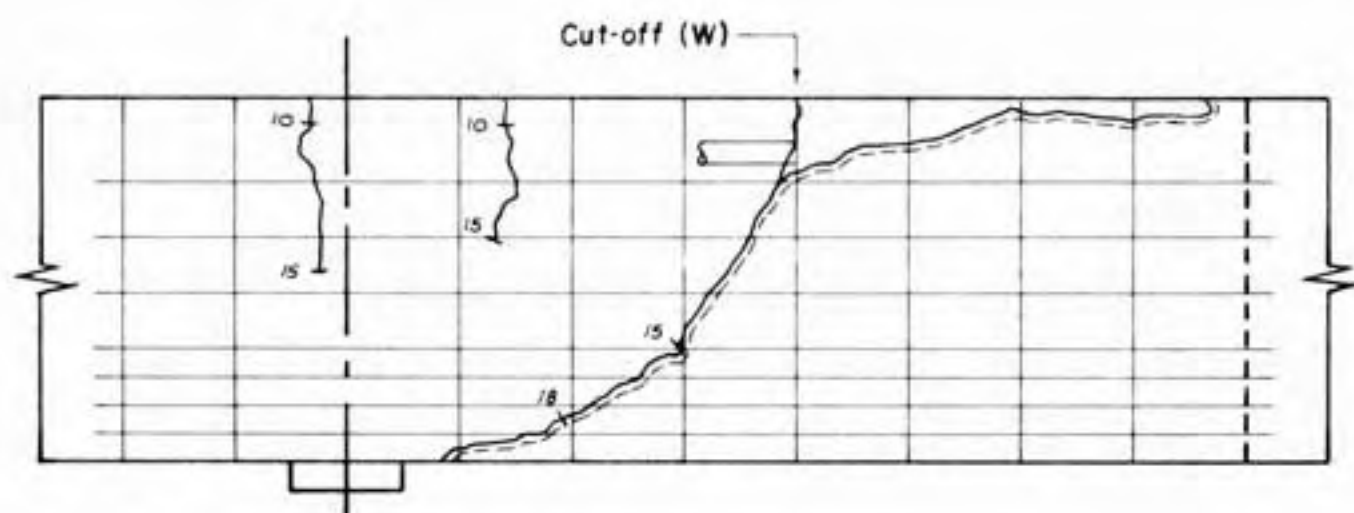


FIGURE 9. LOAD vs. DEFLECTION - SERIES I



EAST SIDE



WEST SIDE

Scale: 1" = 8"

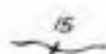
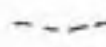
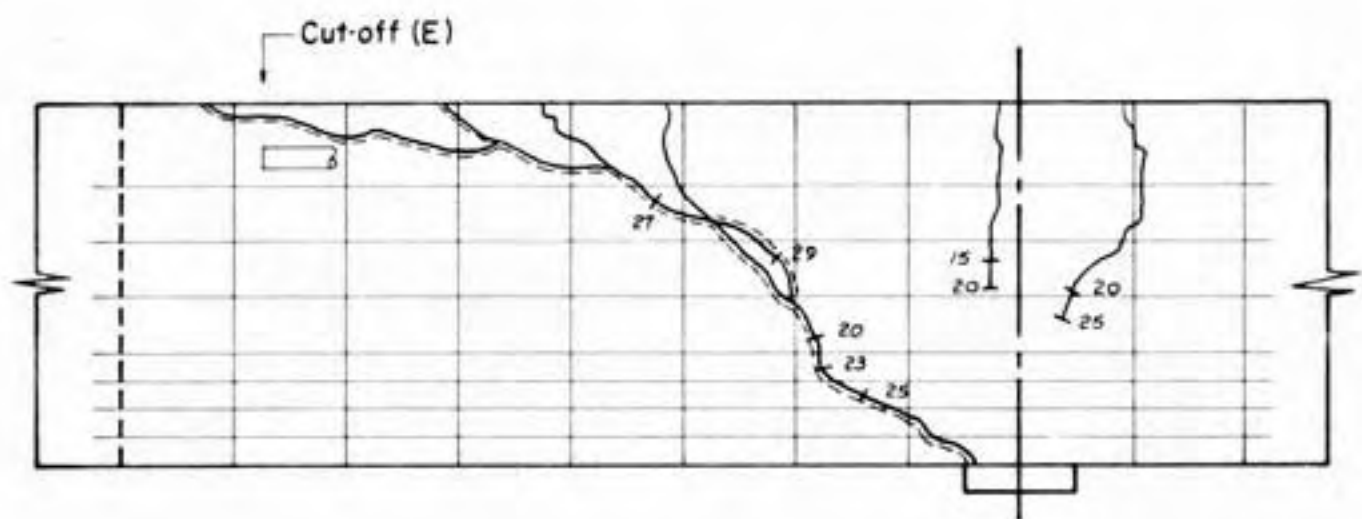
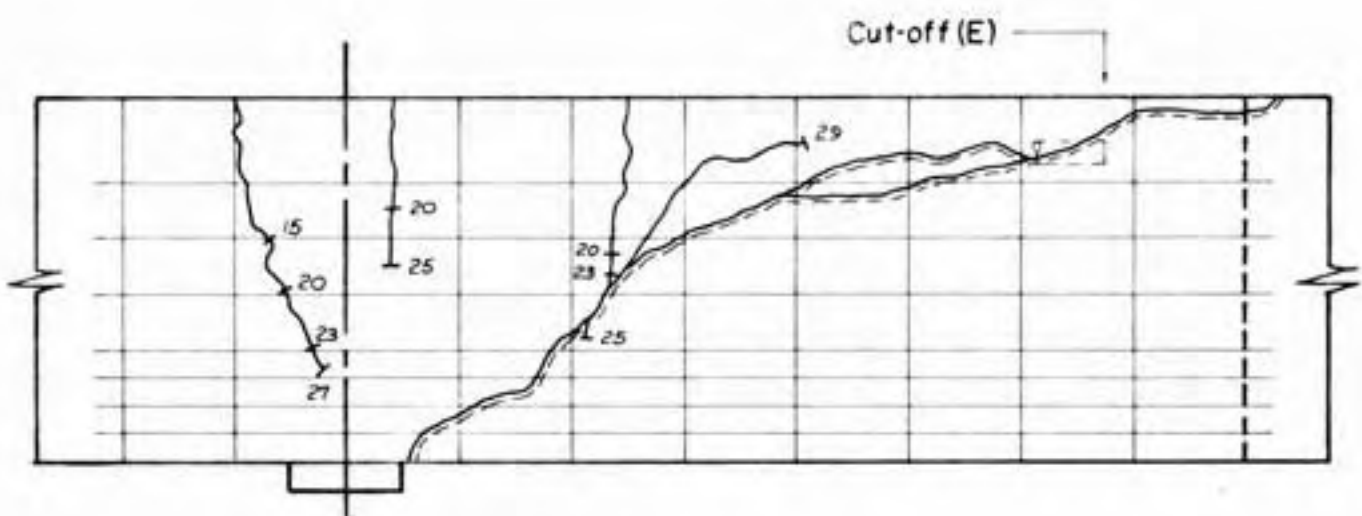
-  Cracks prior to failure
-  Cracks opening wide at failure

FIGURE 10. BEAM IA

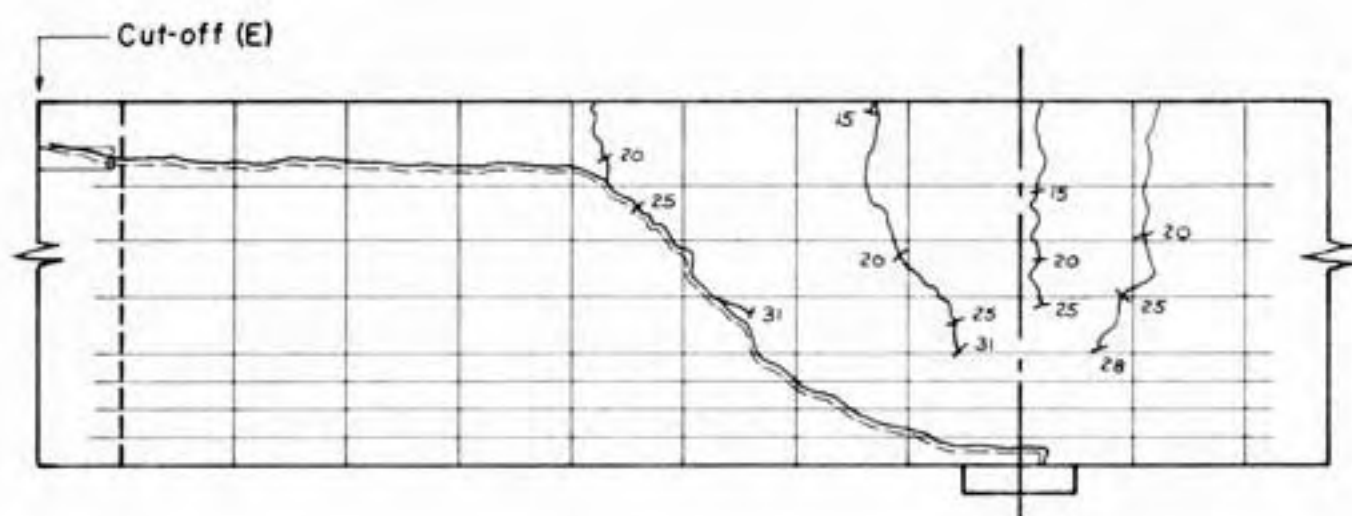


EAST SIDE

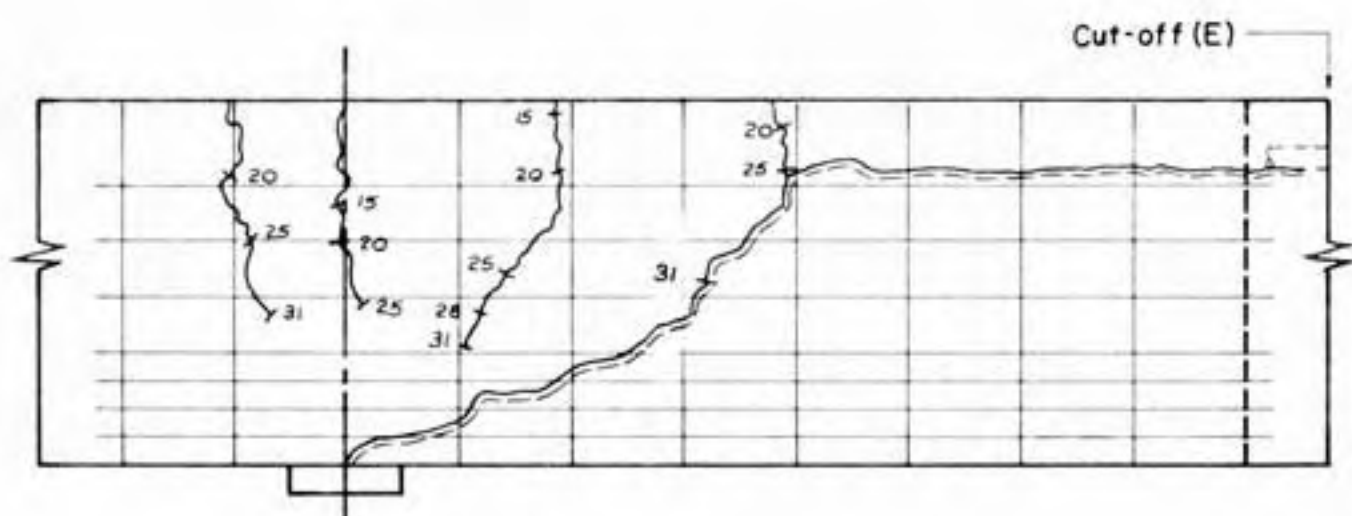


WEST SIDE

FIGURE II. BEAM 1B

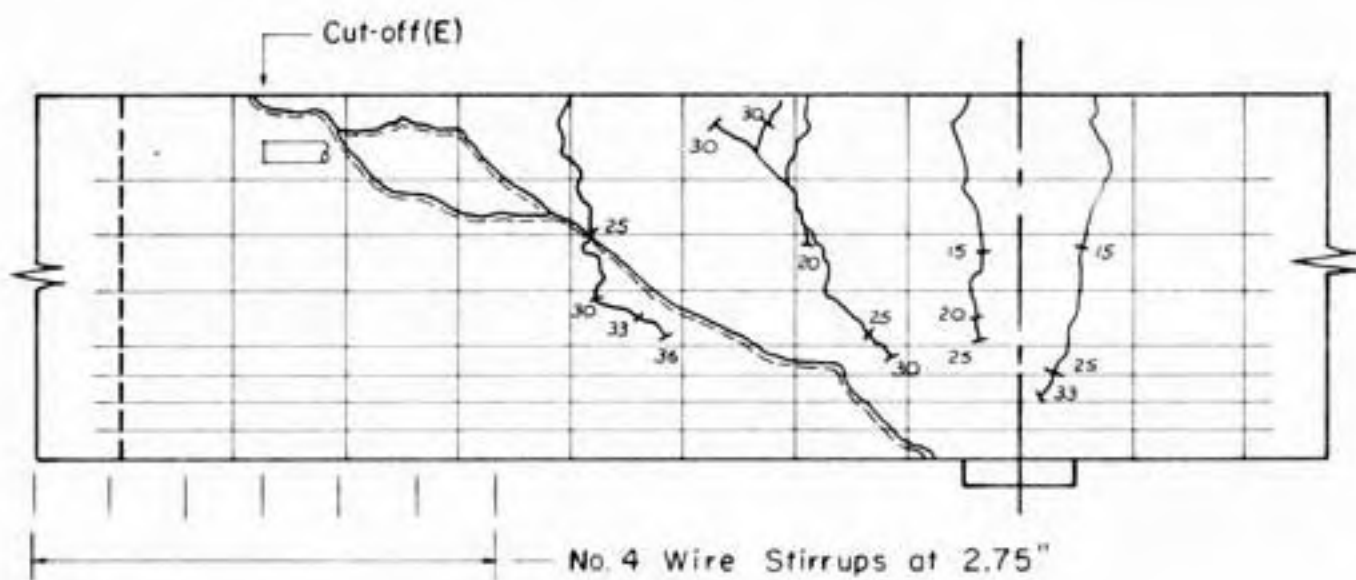


EAST SIDE

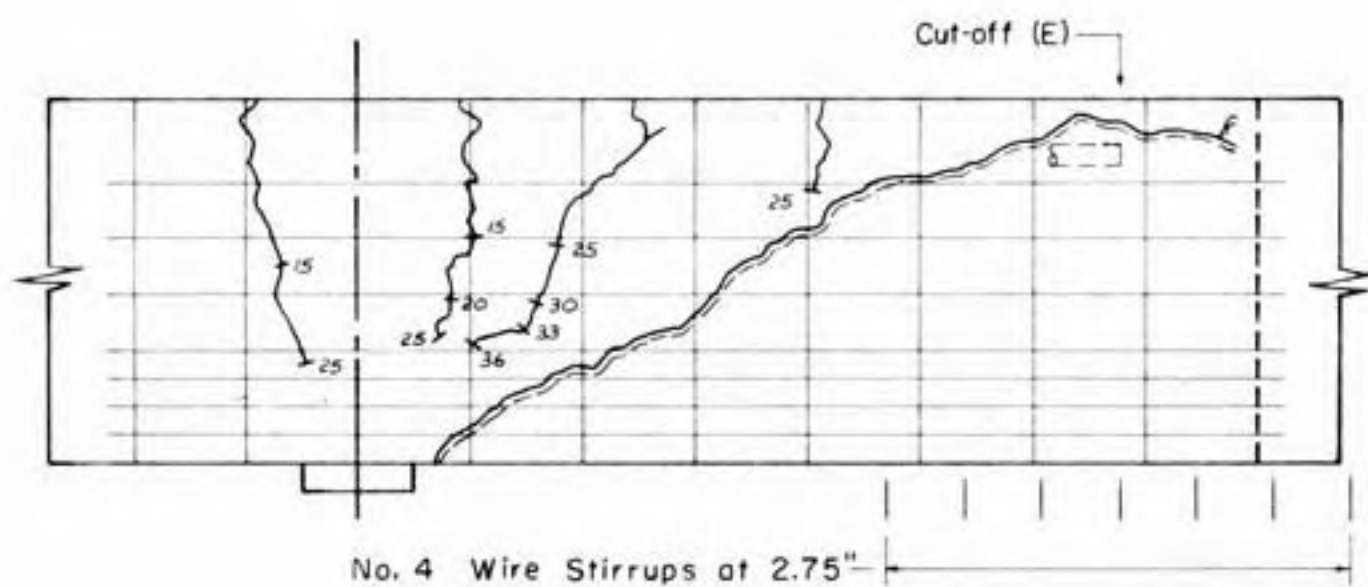


WEST SIDE

FIGURE 12. BEAM IC



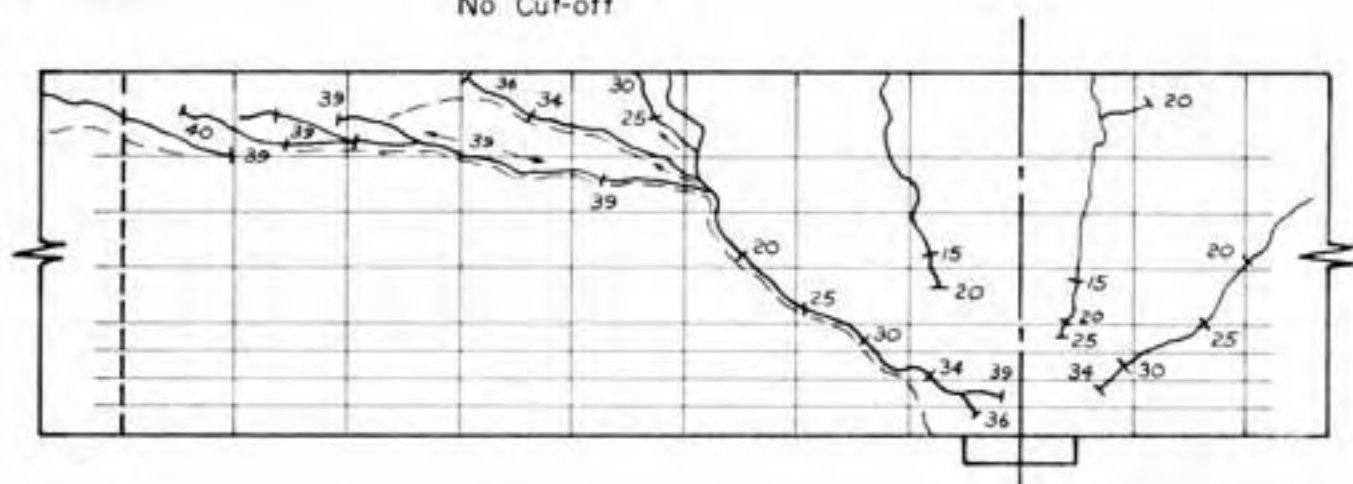
EAST SIDE



WEST SIDE

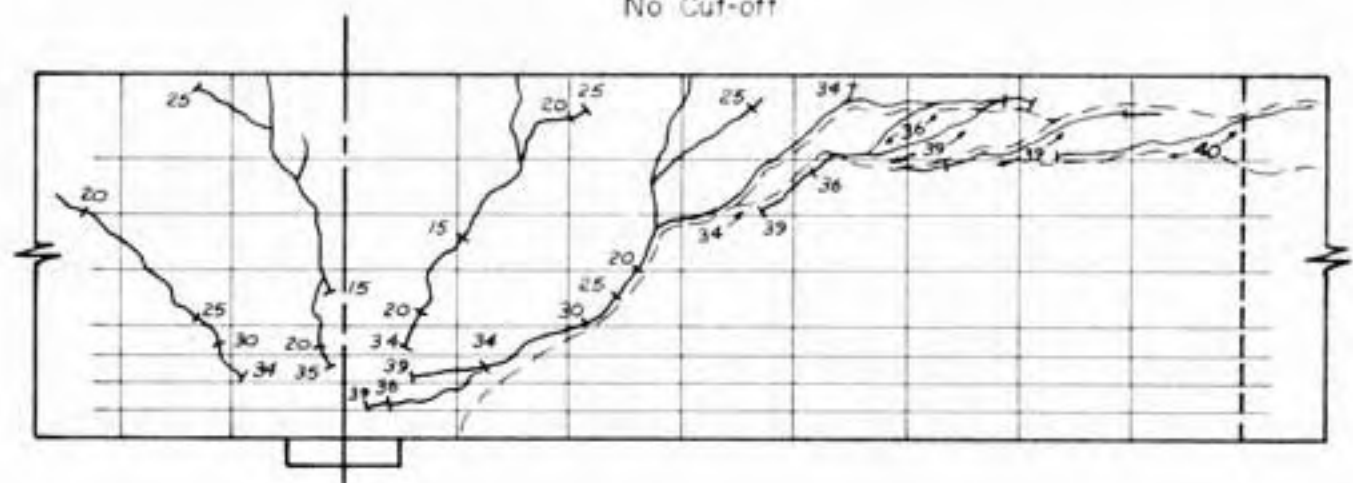
FIGURE 13. BEAM ID

No Cut-off



EAST SIDE

No Cut-off



WEST SIDE

FIGURE 14. BEAM IE

Series II

Beam IIA

By 20^k the beam had developed flexural cracks to the extent that all steel strain gages had indicated steel strain take-up (Figures 18 and 20). In addition, the critical diagonal tension crack had formed as an extension of a flexural crack at Gage 2 and was well into the compression zone on the west side. The steel strain at Gage 2 had already exceeded that of Gage 1. By 30^k , the diagonal tension crack had progressed to within $1\frac{1}{2}$ " of the compression face on both sides. By 32^k the steel strain at Gage 2 had reached yield and the strains at Gages 1 and 3 were approximately equal and one-half of Gage 2. This steel strain phenomenon continued until the beam failed at 42^k .

Beam IIB

Four closely spaced diagonal cracks crossed into the compression region at about the same load of 35^k (Figure 21). The two farthest from the support eventually opened wide at failure. One of these cracks was definitely associated with the steel cut-off and had penetrated to within $1\frac{1}{2}$ " of the compressive face at 50^k .

Failure occurred at 59^k with both cracks opening wide and splitting entirely through the beam.

Beam IIC

By 20^k the beam had developed sufficient flexural cracks to allow a strain take-up on Gage 1 (Figures 18 and 22). At 30^k the critical diagonal tension crack had developed as an extension of a flexural crack midway between

Gages 2 and 3 on the east face. By 35^k the critical crack had reached the neutral axis on the east side and was about an inch away on the west side. The crack continued to propagate toward the compression face until at 55^k it also propagated back along the longitudinal steel from the "critical" flexural crack to about the location of Gage 3. At this point the steel strain at Gage 3 began overtaking the steel strain at Gage 2. The beam failed at a load of 58^k as the crack progressed to the compression face. At this load the steel strains at Gages 2 and 3 were almost identical.

Note: At 44.6^k the steel beam used to load the test beam failed and the load was removed. The beam was then reloaded. The concrete and steel strains compared reasonably well. It became apparent that no errors were induced by the failure of the first loading beam and hence, only the strain and deflection data from the reloading were considered.

Beam IID

Two diagonal tension cracks developed, located approximately 10" and 20" from the support (Figure 23). The critical crack crossed the neutral axis at 35^k , but further increase in load (40^k - 50^k) was required to extend it back to the tension steel. Splitting along the longitudinal steel was not prevented by the stirrups, but was delayed and did not extend into the positive moment region until near ultimate load.

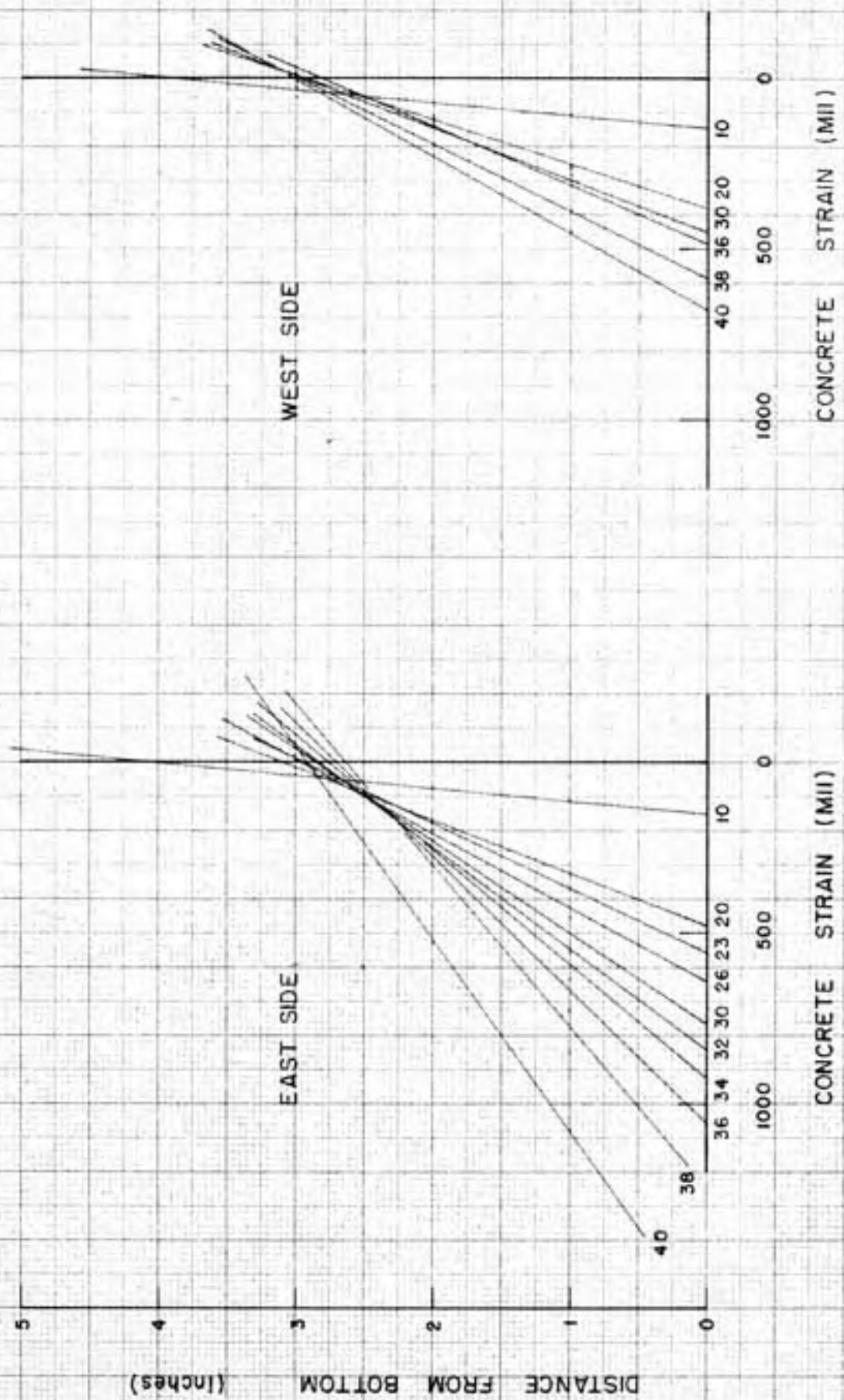


FIGURE 15. CONCRETE STRAIN DISTRIBUTION — BEAM IIA

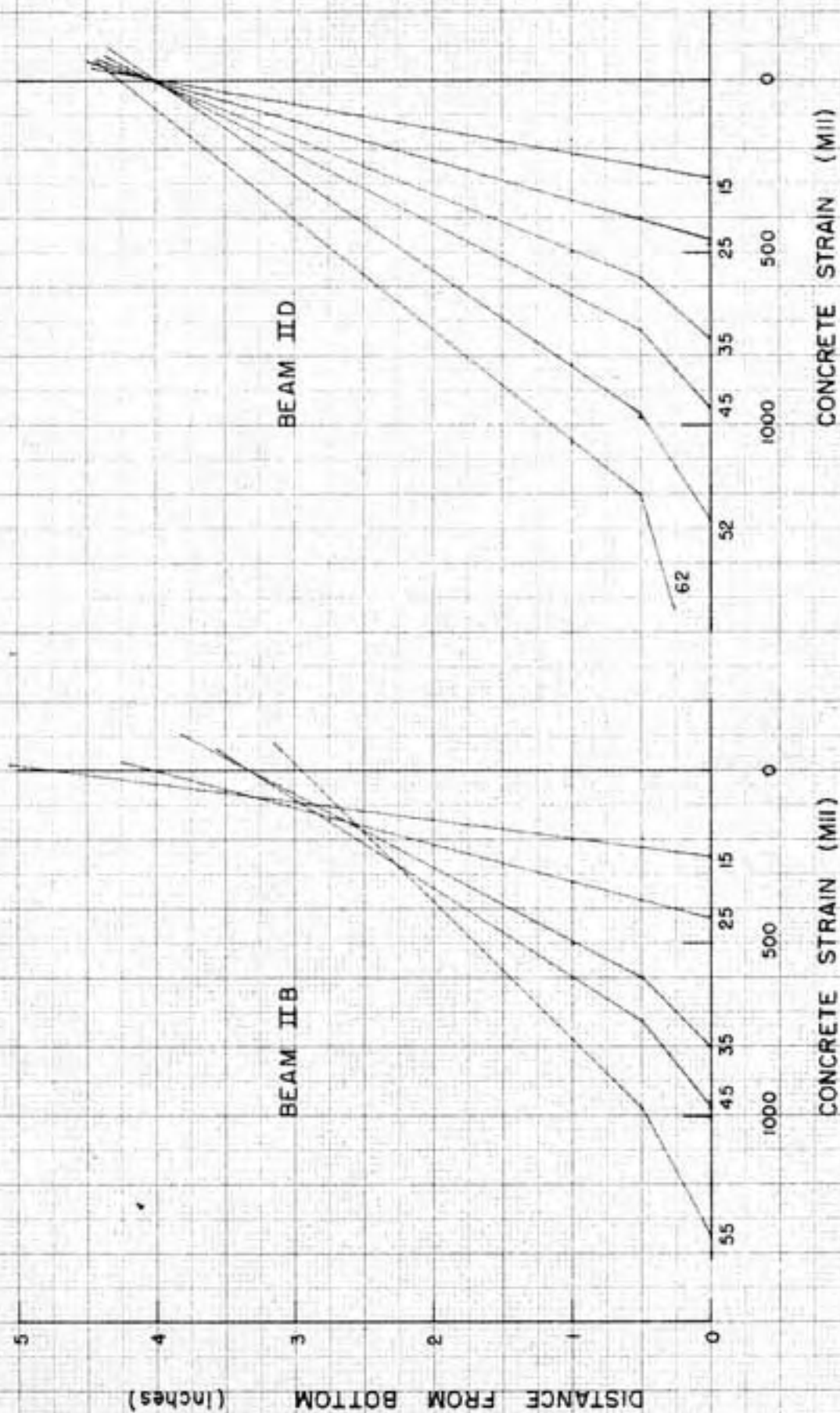


FIGURE 16. CONCRETE STRAIN DISTRIBUTION — BEAMS IIB and IID

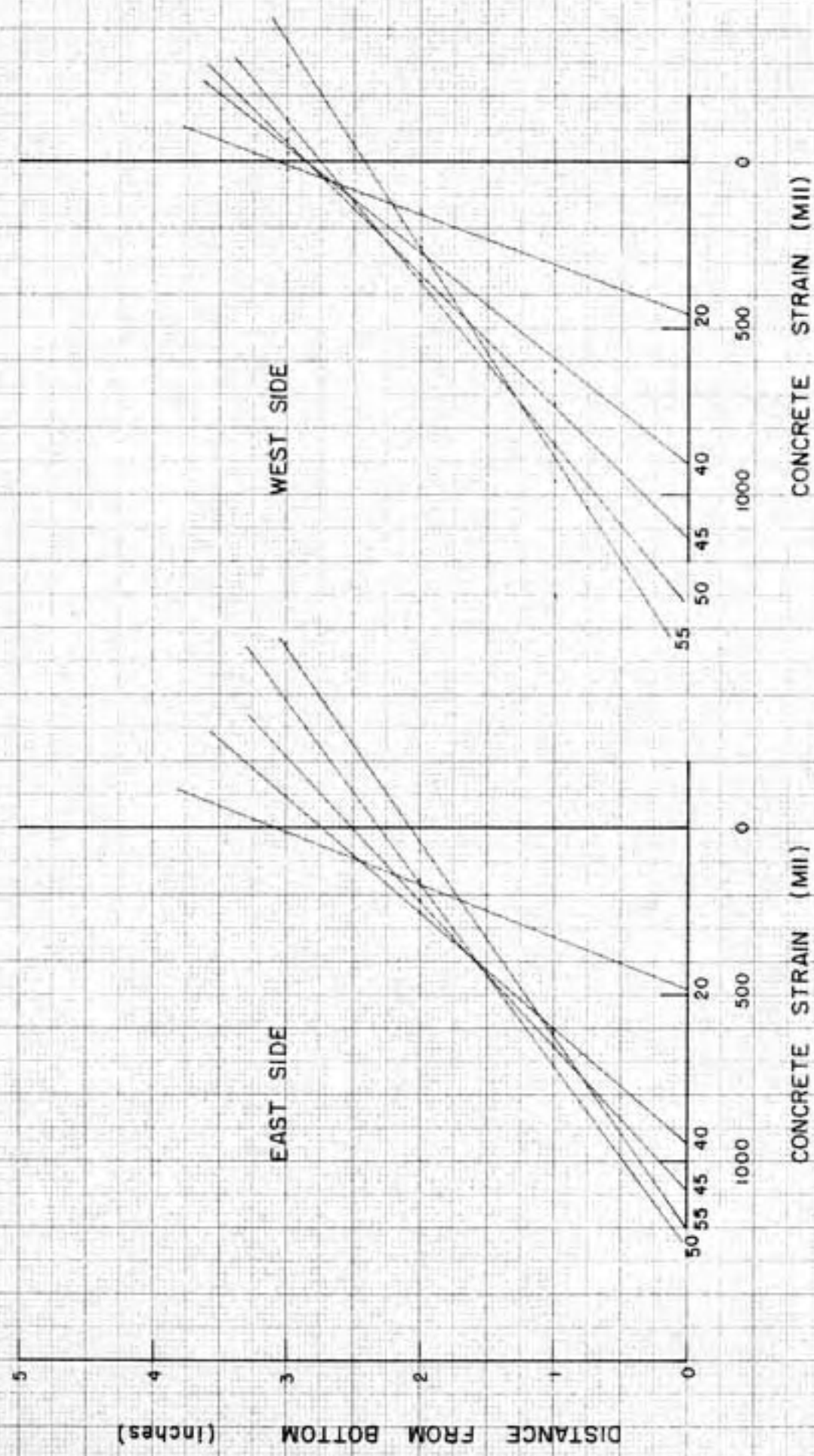


FIGURE 17. CONCRETE STRAIN DISTRIBUTION — BEAM IIC

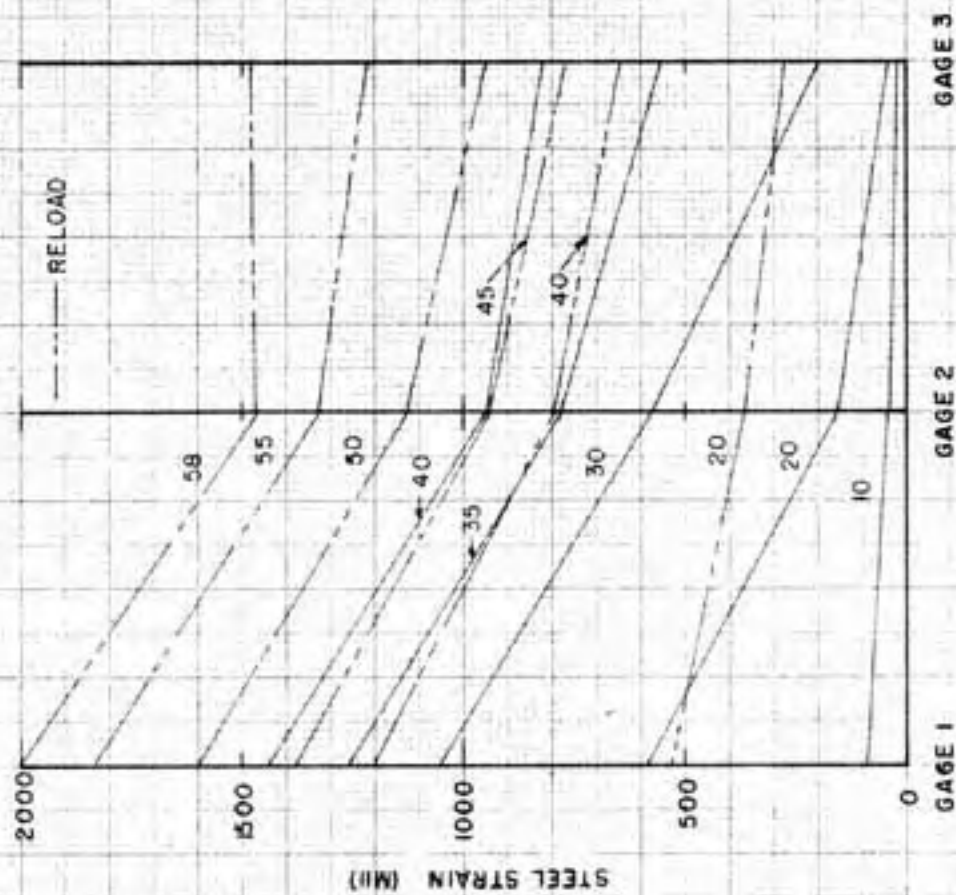
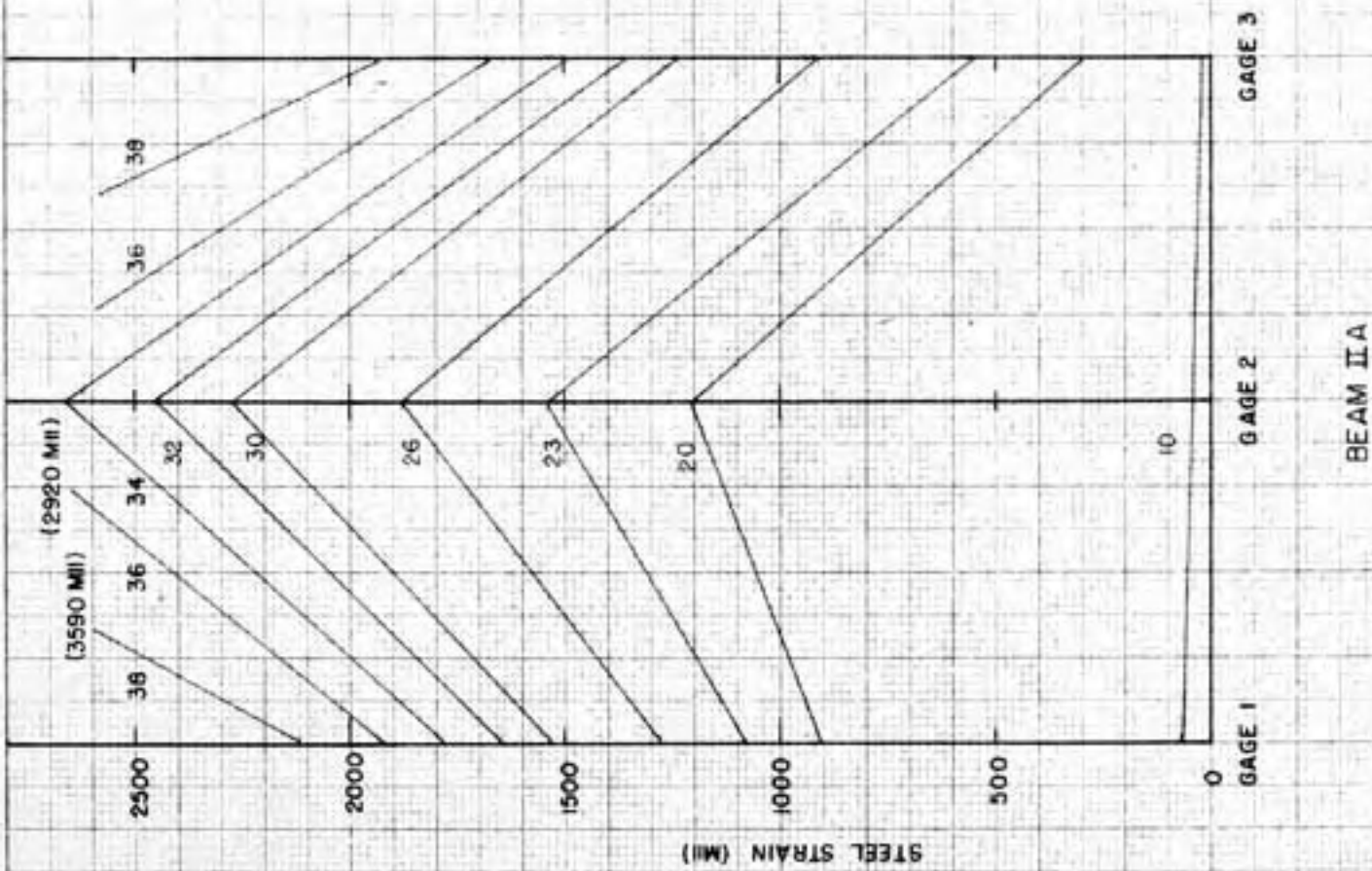


FIGURE 18. STEEL STRAIN vs. GAGE LOCATION — BEAMS IIA and IIC

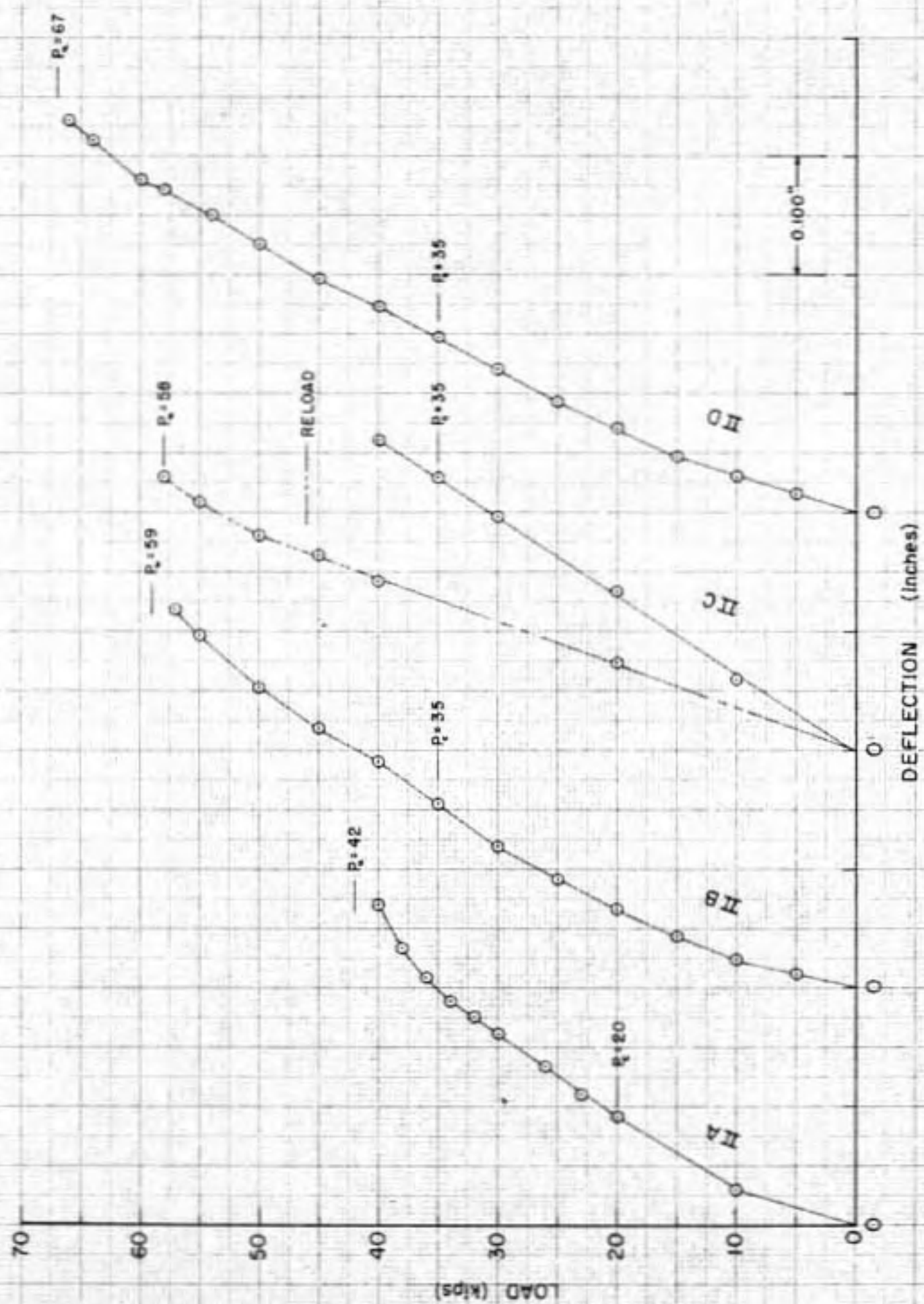


FIGURE 19. LOAD vs. DEFLECTION - SERIES II

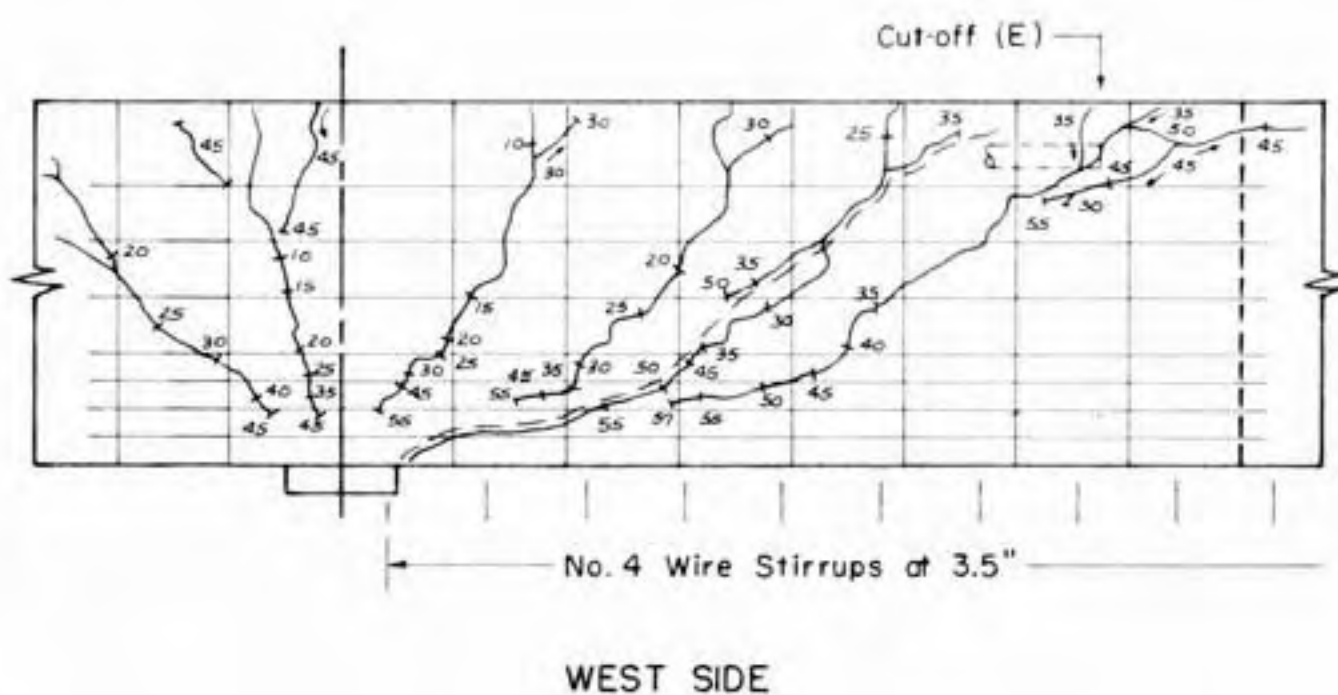
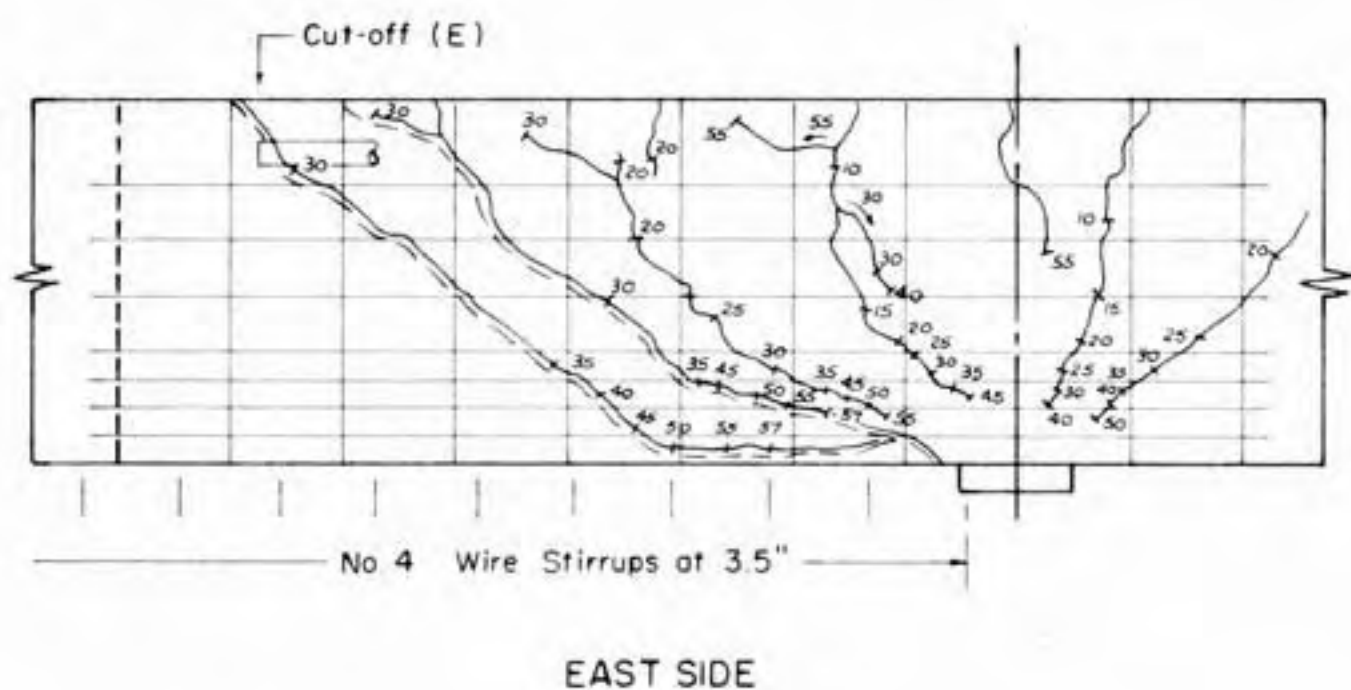


FIGURE 21. BEAM II B

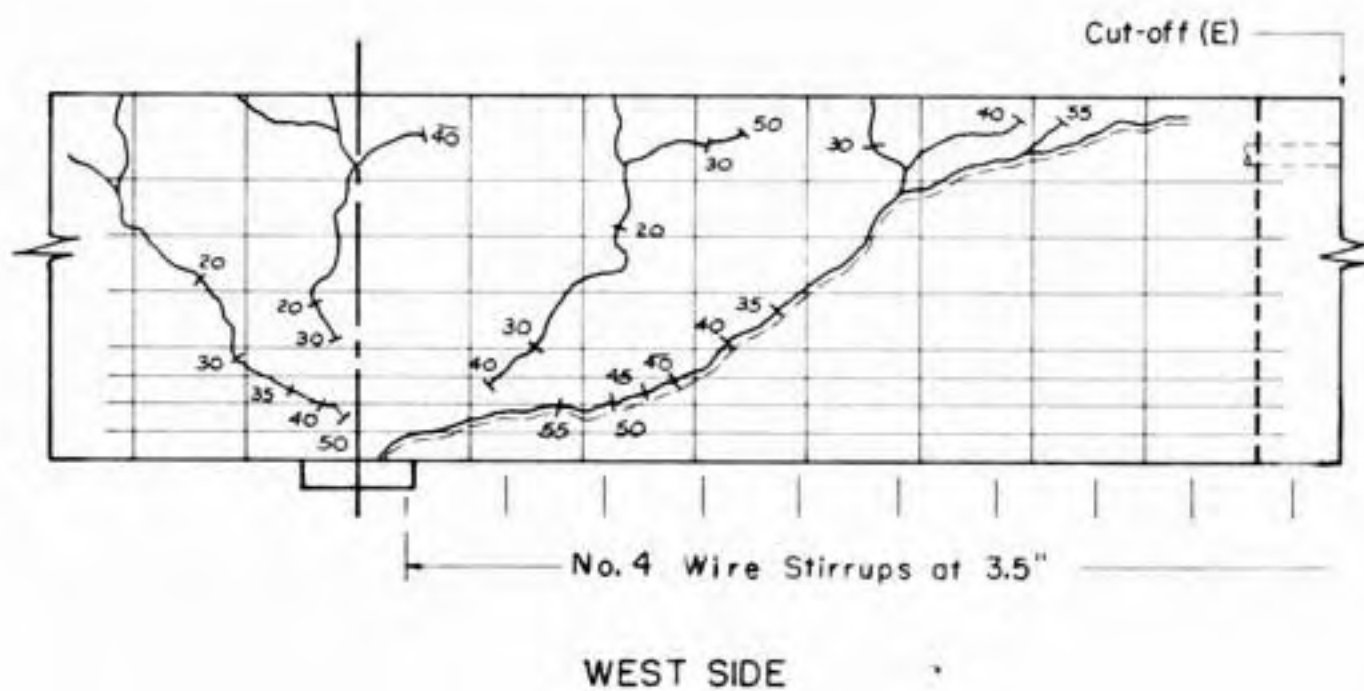
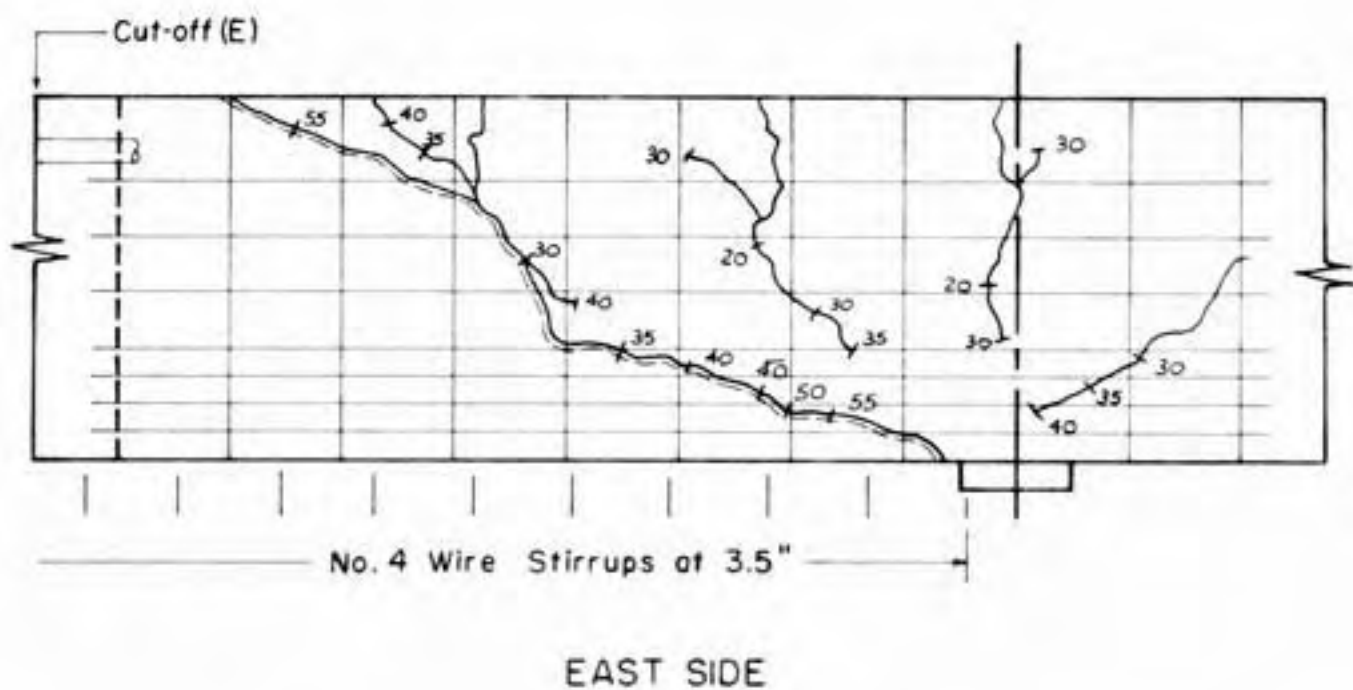
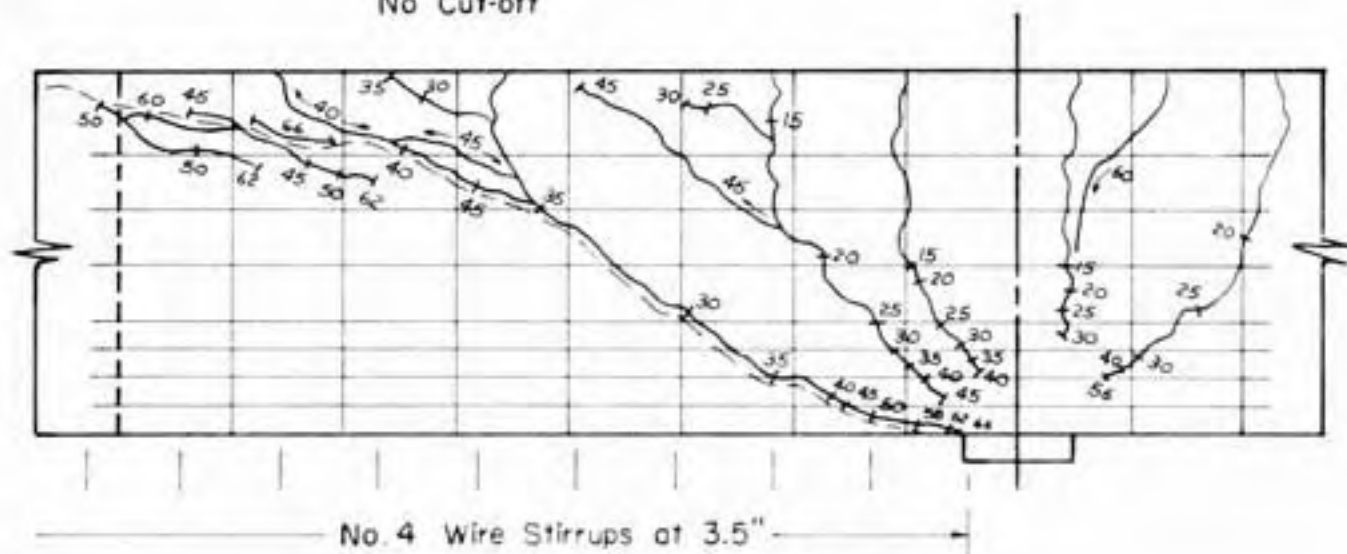


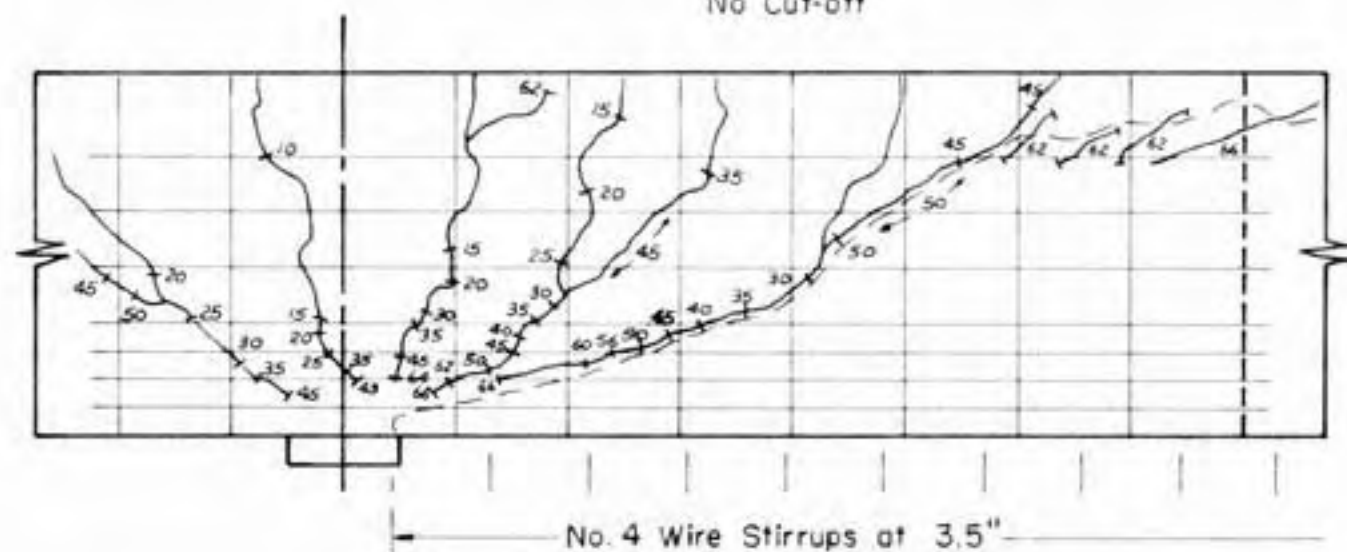
FIGURE 22. BEAM IIC

No Cut-off



EAST SIDE

No Cut-off



WEST SIDE

FIGURE 23. BEAM IID

Series III

Beam IIIA (IB)

Flexural cracks had produced a strain take-up in Gage 1 by a load of 20^k (Figures 7 and 11). The critical diagonal tension crack had already developed as an extension of a flexural crack on the east side of the beam midway between Gages 1 and 2 and had propagated to within an inch of the neutral axis. The diagonal tension crack crossed the neutral axis at 23^k . The steel strain at Gage 2 had almost overtaken the steel strain at Gage 1 at 27^k . The beam failed at 31^k as the diagonal tension crack propagated back to the longitudinal steel and then continued along it.

Beam IIIB

The diagonal crack formed at 25^k along the same path as IIIA (Figure 27). At 29.1^k the crack was within $1/2"$ of the bottom and splitting occurred along the steel to the cut-off. The load fell suddenly to 25.3^k . Load was again increased to 27^k at which time both top bars split out and the beam fell in two pieces.

Beam IIIC

Flexural cracks produced strain take-up in Gage 1 by 15^k (Figures 25 and 28). By 25^k several flexural cracks had opened on each side but no diagonal tension crack had formed. The steel strains also remained in the proper ratio. Then at 29^k the beam failed suddenly as a diagonal tension crack propagated from the support point to the cut-off point and then along the continuing bar to its cut-off point.

Beam IIID

The beam developed flexural cracks and failed in approximately the same manner as IIIC (Figure 29). The failure load was 32^k .

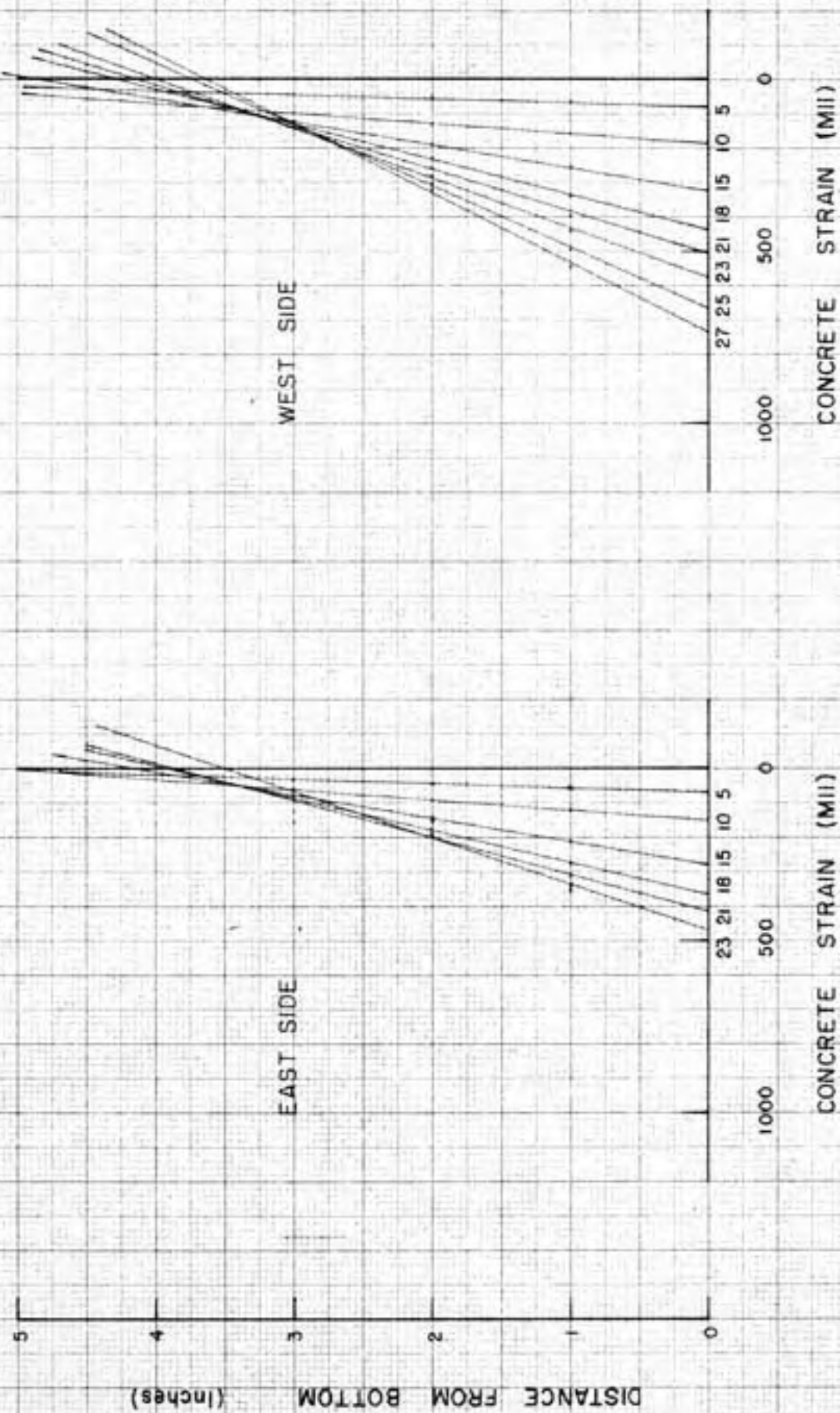


FIGURE 24. CONCRETE STRAIN DISTRIBUTION — BEAM III C

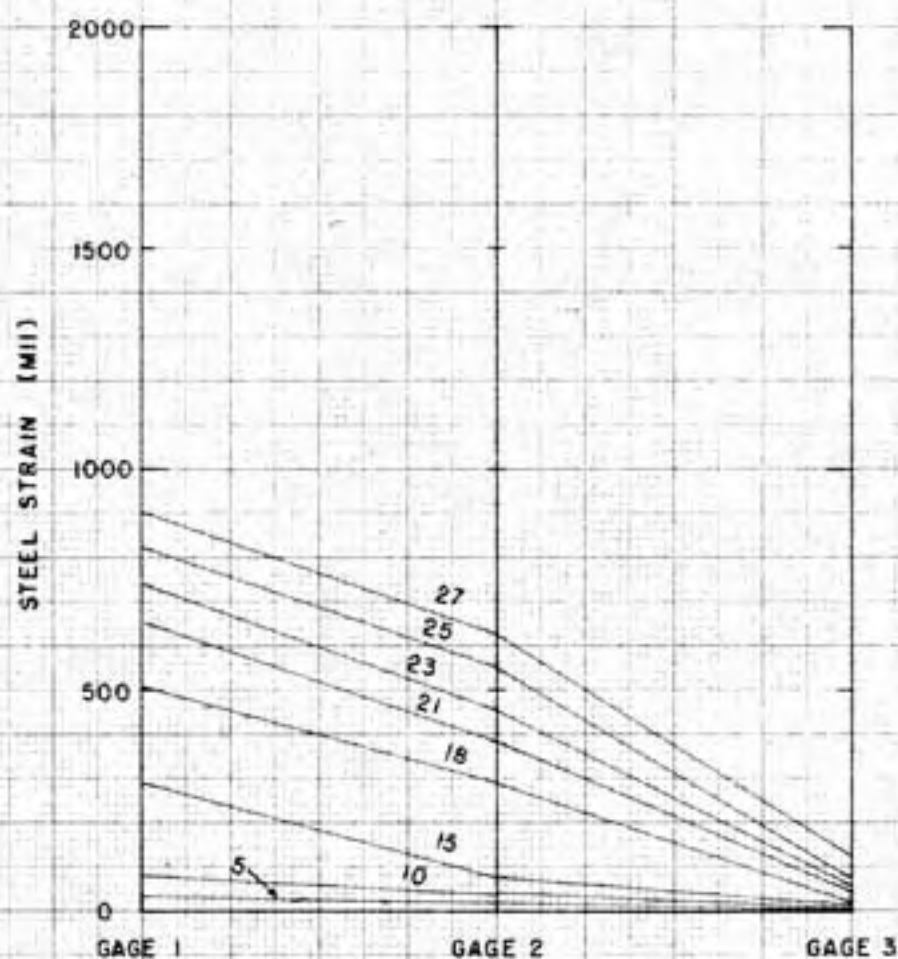


FIGURE 25. STEEL STRAIN vs. GAGE LOCATION — BEAM IIC

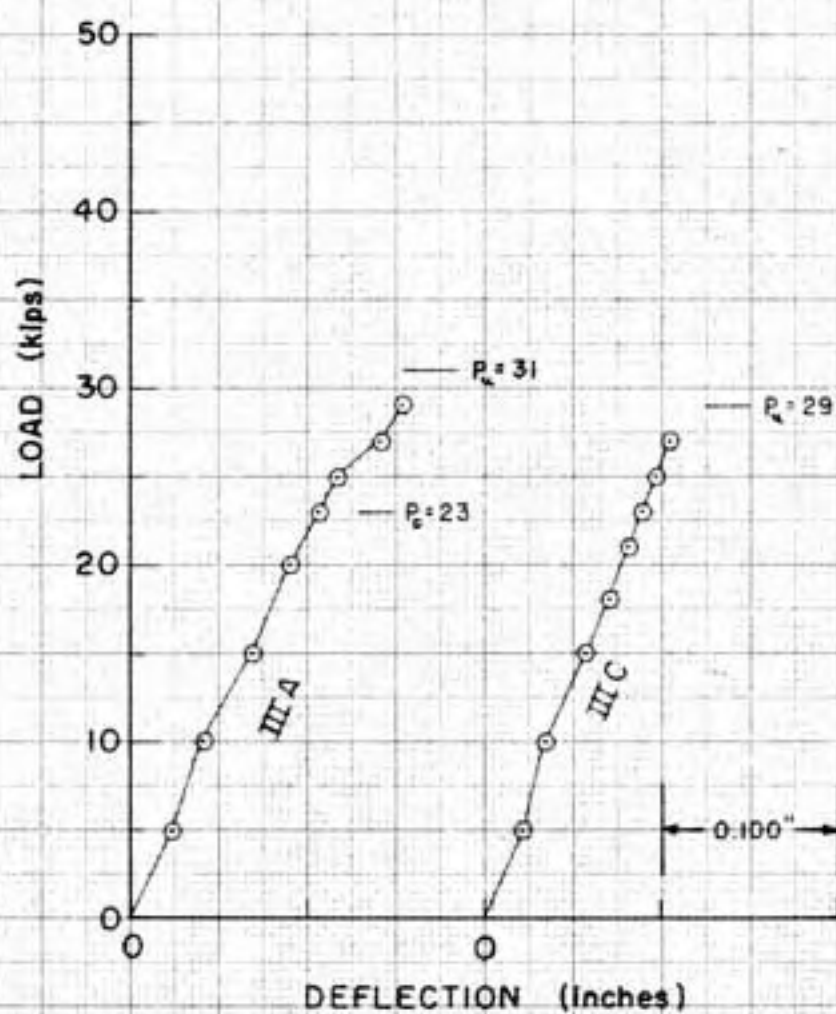
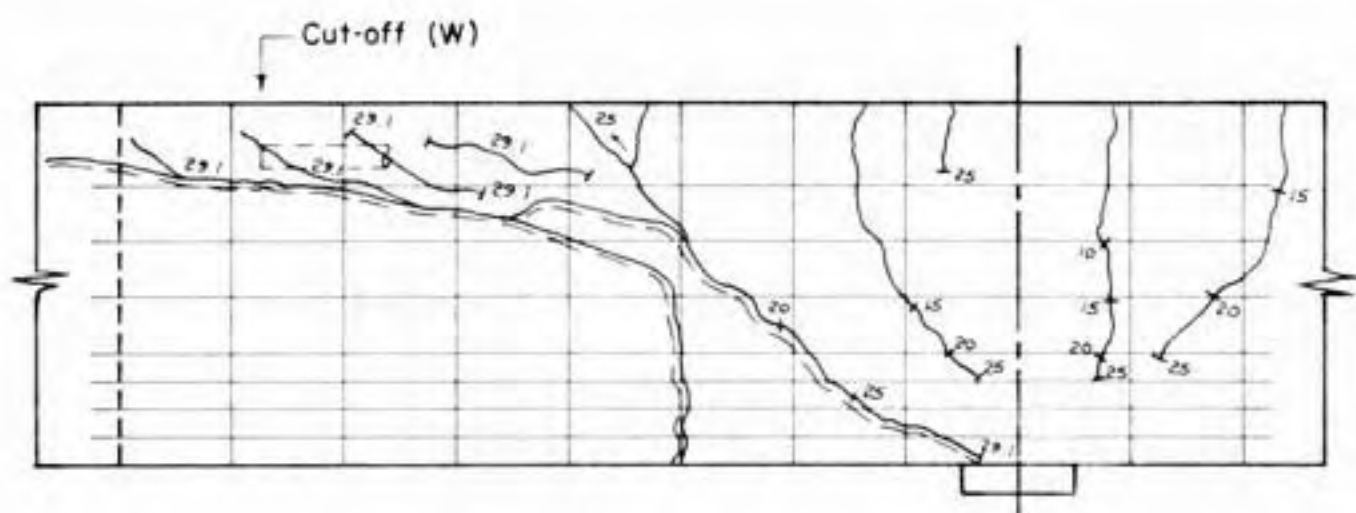
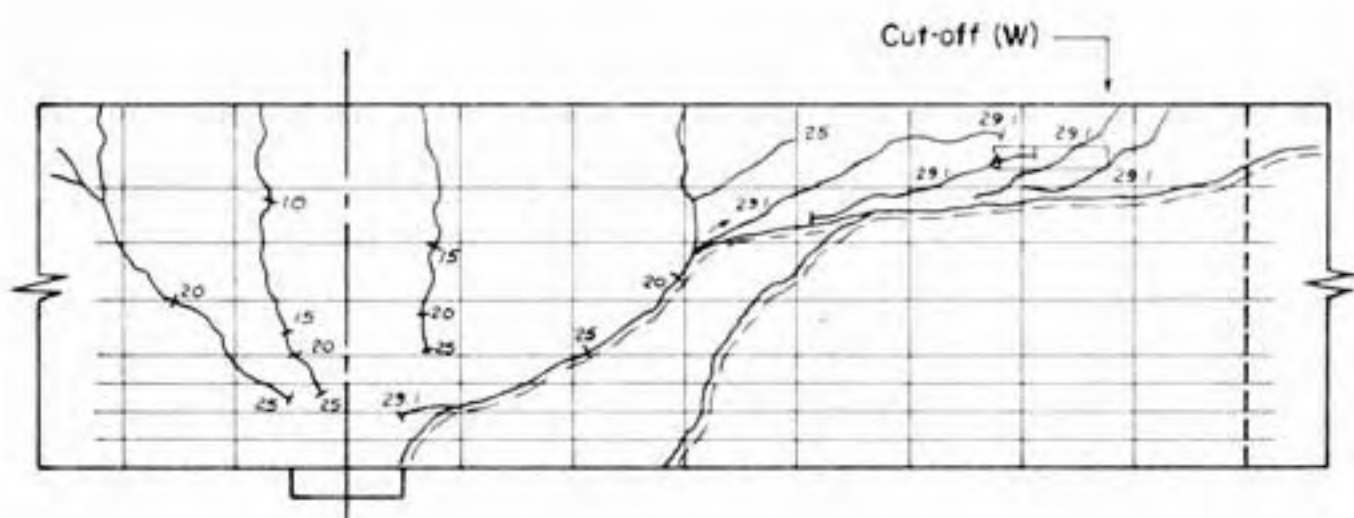


FIGURE 26. LOAD vs. DEFLECTION — SERIES III



EAST SIDE



WEST SIDE

Scale: 1" = 8"

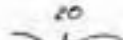

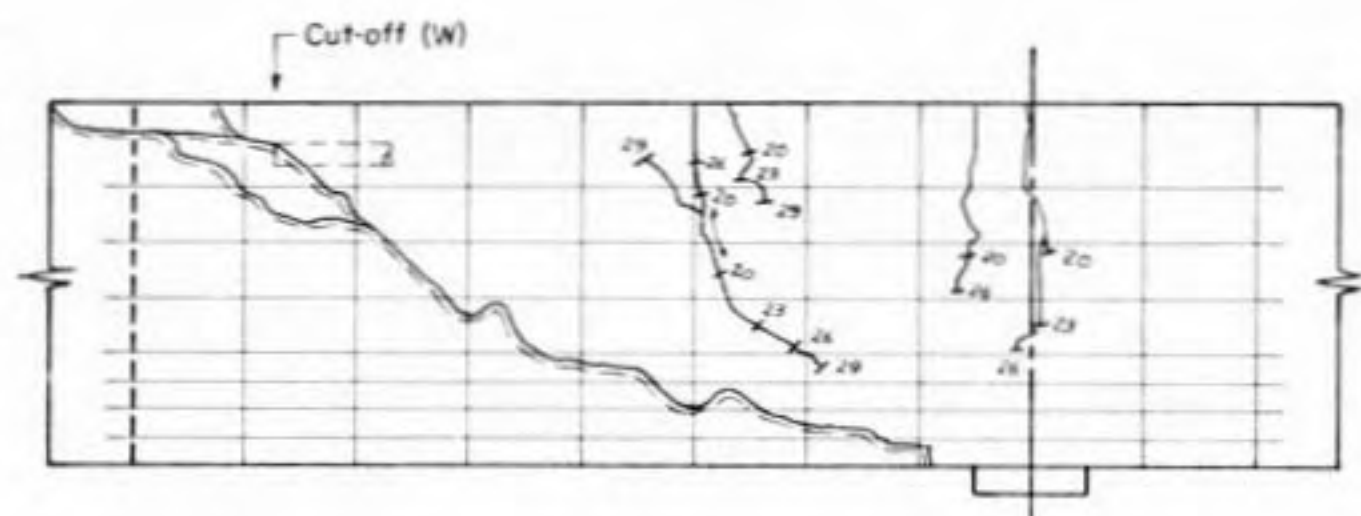
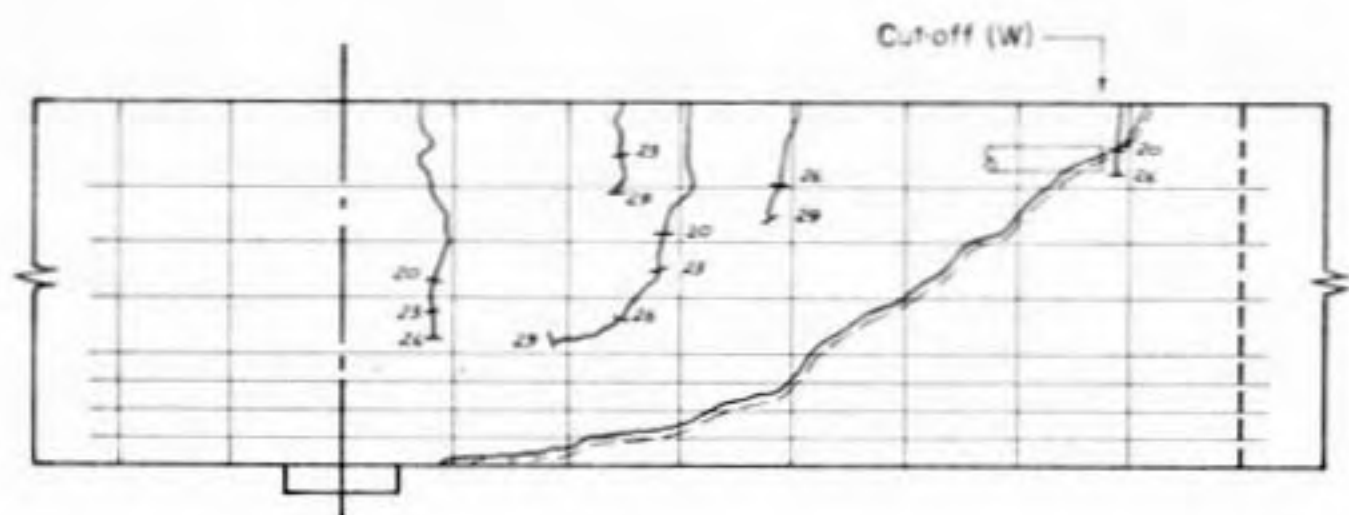
-  Cracks prior to failure
-  Cracks opening wide at failure

FIGURE 27. BEAM III B



EAST SIDE



WEST SIDE

FIGURE 29. BEAM III D

DISCUSSION OF TEST RESULTS

Mode of Failure

In all the beams tested - with the exception of Beams IE and IID - the mode of failure was by diagonal tension. The mode of failure for Series I and II was that of a diagonal tension crack propagating as an extension of a flexural crack. In Series III, the mode of failure was also by diagonal tension; however, in the beams having the lower strength concrete, the critical diagonal tension crack was not formed until failure.

The two exceptions noted were the beams having none of the longitudinal steel cut off. These two beams failed in the shear-compression mode.

Beams Without Web Reinforcement

(Series I)

Beams IA, IB, IC, and IE developed their critical diagonal cracks as an extension of a flexural crack approximately midway in the shear span (Figures 10, 11, 12, 14). At failure, the diagonal tension crack propagated back along the remaining negative reinforcement bar for some distance.

Beam ID (Figure 13) did not have a diagonal tension crack form until failure. However, the crack did propagate along the remaining negative reinforcement bar toward the cut-off point at failure.

Beams With Reinforcement

(Series II)

Beams IIB, IIC, and IID developed their diagonal tension cracks similarly as an extension of a flexural crack (Figures 21-23). The diagonal cracking load was also the same in each of the three beams. Moreover, the ultimate

loads of Beams IIB and IIC were almost identical (Table 3).

Beam IIA, however, did not behave in the same way. The critical diagonal tension crack developed as an immediate extension of a flexural crack (Figure 20) and both the diagonal cracking load and the ultimate load were substantially lower than the corresponding load for any of the other three beams in the series (Table 3).

Effect of Concrete Strength

(Series III)

The basis for Series III beams was the discrepancy between the AASHTO and ACI allowable shear strengths, particularly in the neighborhood of $f_c^0 = 3000$ psi (See Figure 30 which shows the comparison for the beams of this test program). It was thought that this discrepancy would produce an even smaller factor of safety in AASHTO cut-off requirements.

Beams IIIA and IIIB had the higher concrete strength. Both beams developed their critical diagonal tension cracks as an extension of a flexural crack (Figures 11 and 27). The crack then propagated back along the remaining negative reinforcement bar at failure as in Series I.

Beams IIIC and IIID had the lower strength. Their diagonal tension cracks did not form until failure and were independent of any flexural crack (Figure 28 and 29).

Factors Affecting Beam Behavior

In addition to measuring the load carrying capacity of the beams as it was affected by the location of bar cut-off, instrumentation was also used to measure the effect of cut-off upon the steel strain of the remaining bar,

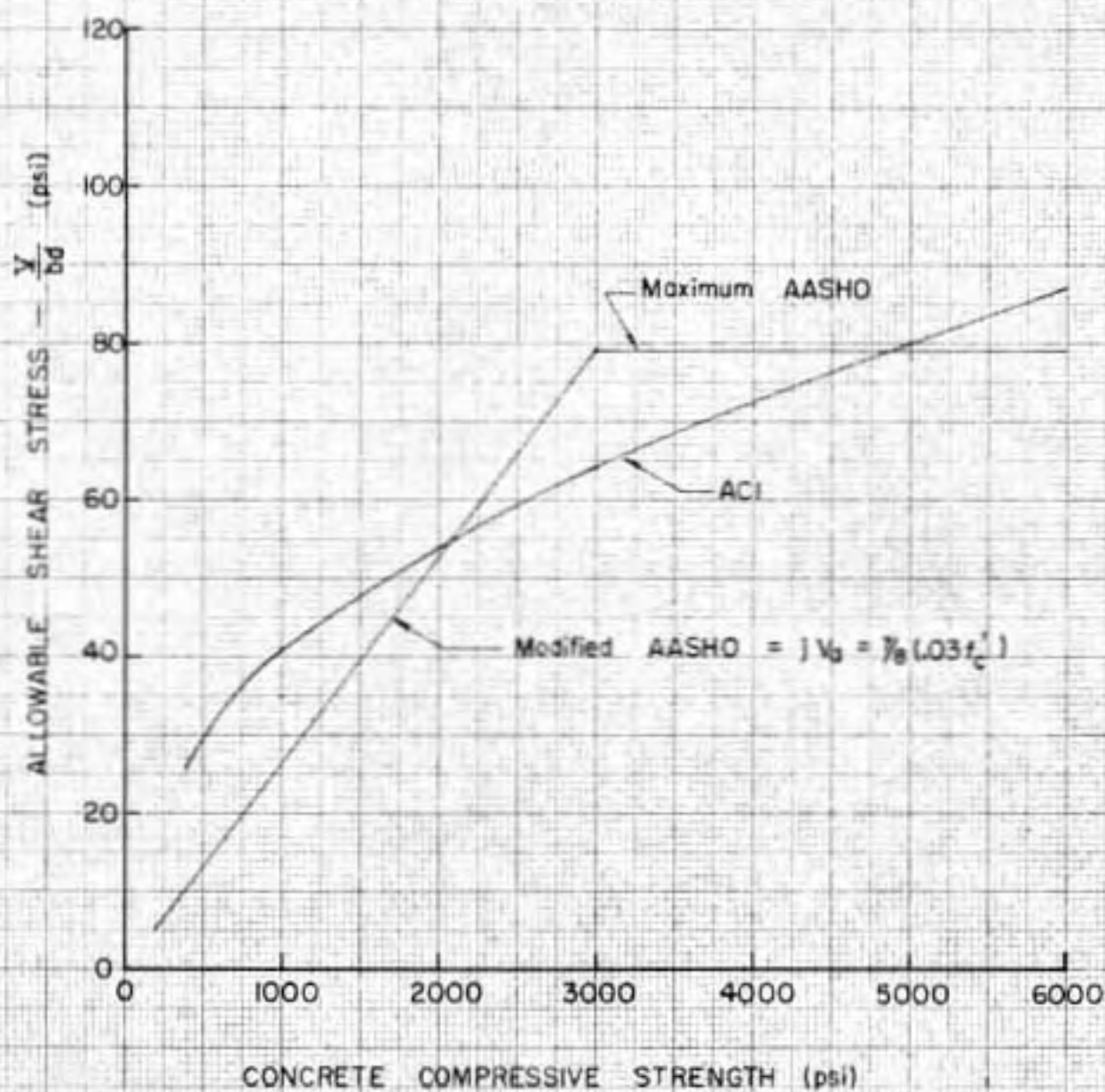


FIGURE 30. COMPARISON OF AASHTO AND ACI ALLOWABLE SHEAR STRENGTHS FOR BEAMS WITHOUT WEB REINFORCEMENT

unsymmetrical bending due to the change in cross section beyond the cut-off, and beam stiffness as reflected by deflections.

Steel Strain

Stress redistribution may be induced in the longitudinal reinforcement due to diagonal cracking. The formation of the diagonal crack requires the longitudinal reinforcing steel at section b-b (Figure 31) to resist the greater external moment at section a-a, as shown by summation of moments about the centroid of compression in the uncracked portion (section a-a).

Series I Beams The stress redistribution occurred at Gage 2, in Beams IA, IB, IC, and ID, as soon as the critical diagonal tension crack crossed the neutral axis. However, in the first two beams the redistribution continued to increase substantially until beam failure, (Figure 7), whereas in Beams IC and ID the redistribution remained relatively small (Figure 8).

Series II Beams Extensive redistribution occurred in Beam IIA at Gage 2 after the diagonal tension crack had formed (Figure 18). Redistribution also occurred in Beam IIC at Gage 3 after the diagonal tension crack had propagated out to Gage 3 (Figure 18).

Series III Beams Redistribution occurred in Beam IIIA (IB) at Gage 2 after the diagonal crack had progressed through the neutral axis (Figure 7). This redistribution increased somewhat until failure. However, no appreciable redistribution occurred in Beam IIIC (Figure 25). This beam failed suddenly upon formation of the critical diagonal tension crack.

Unsymmetrical Bending

Unsymmetrical bending can occur due to the resulting "unsymmetrical" section caused by the bar cut-off. The diagonal tension crack is resisted

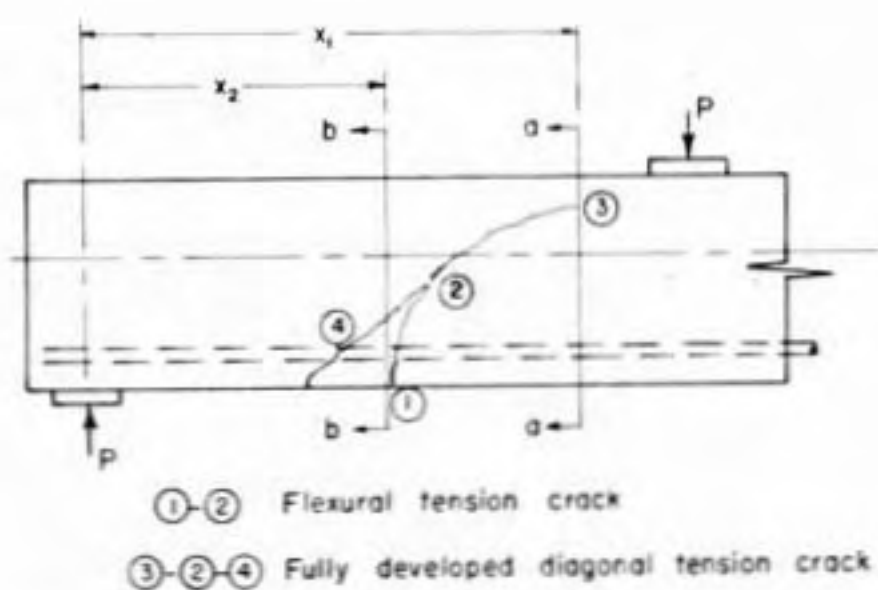
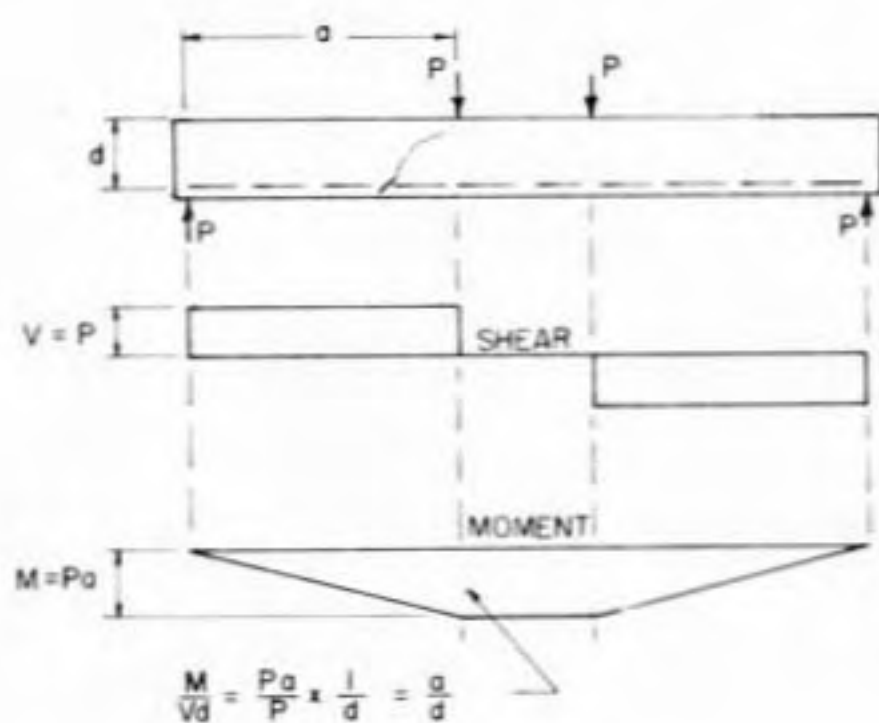


FIGURE 31. FORMATION OF DIAGONAL TENSION CRACK

more on the side of the remaining bar, and hence, the uncracked section will be trapezoidal with larger concrete strains on the side of the remaining bar (Figure 32).

This hypothesis is shown in the Series I beams with the exception of ID and IE (Figures 2-6). In these beams, (IA, IB, IC), the concrete strains were much larger and the neutral axis lower on the side of the remaining bar.

In the Series II beams, with the exception of Beam IIA, the presence of stirrups resisted the diagonal tension crack and its tendency to produce the unsymmetrical bending (Figures 15-17). However, the concrete strains of Beam IIA indicated that unsymmetrical bending was present.

In Series III beams, the concrete strains of Beam IIIA (IB) (Figure 3) showed unsymmetrical bending, whereas the concrete strains of Beam IIIC remained much more uniform until failure (Figure 24).

Beam Stiffness

The deflection of a beam is in direct proportion to its stiffness. Hence, the effect of diagonal tension cracking upon beam stiffness may be measured by load deflection plots.

The beam stiffness was not affected substantially in any of the series by diagonal tension cracking with the exception of the beams with the theoretical cut-off (IA and IIA) (Figures 9, 19, 26). Beams IA and IIA indicated much greater deflections for a given load almost immediately after loading had begun.

Analysis of Test Results

Nominal Shear Stress at Diagonal Cracking

The expression recommended by ACI-ASCE Committee 326 (1) for predicting

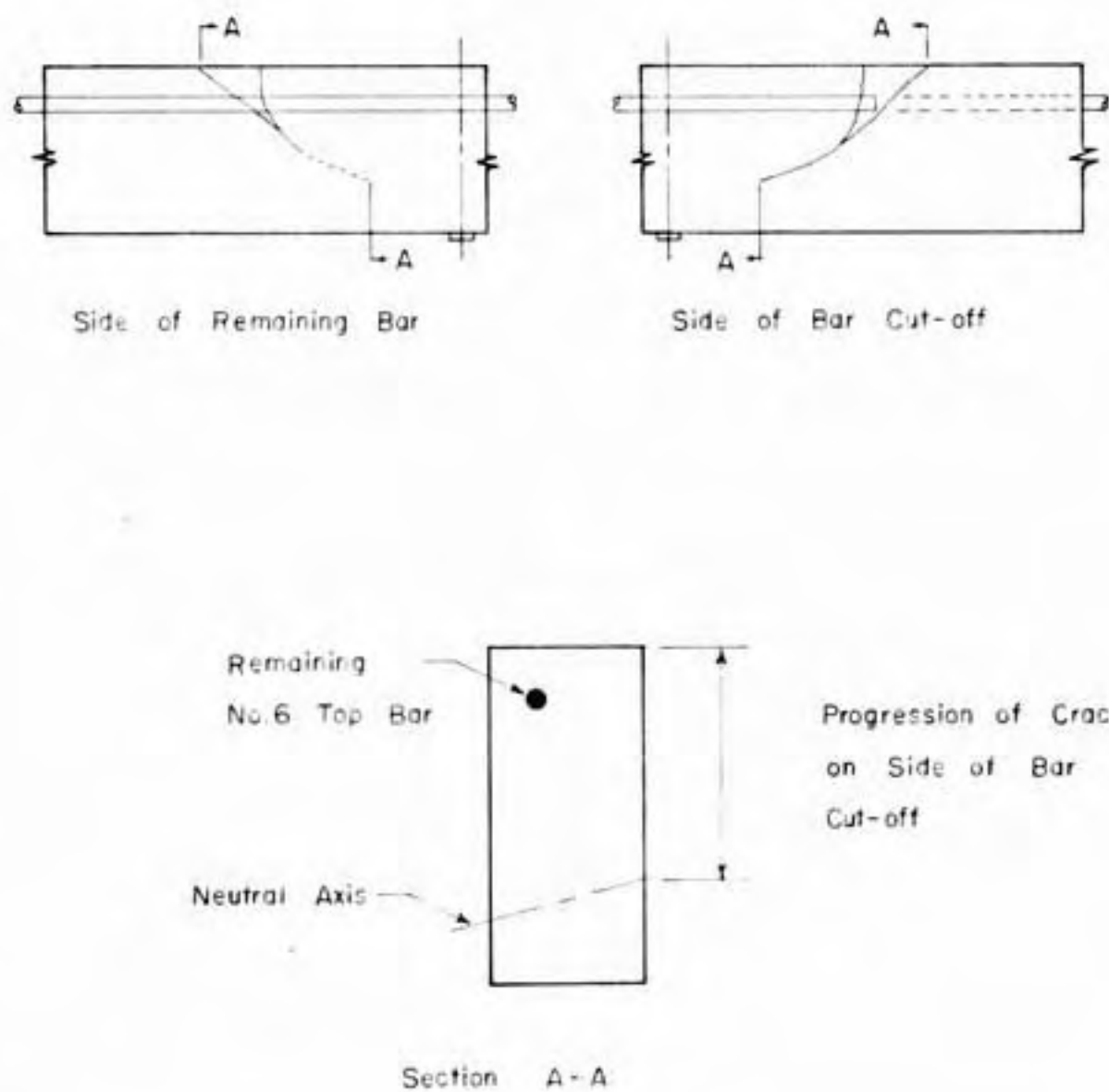


FIGURE 32. DEVELOPMENT OF UNSYMMETRICAL BENDING

the resistance to diagonal tension cracking has been shown to give good results under a variety of conditions. This equation is:

$$v_c = \frac{V}{bd} = 1.9 \sqrt{f'_c} + 2500 \frac{pVd}{M}$$

This equation is intended to predict the average shearing stress required to produce diagonal cracking at the section considered. For the beams of this study the critical section is at a distance of one effective depth, d , from the section of maximum moment. Hence, $\frac{V}{M} = \frac{1}{x-d}$ for these beams. Test results are compared with values predicted by this equation in Table (4).

For the beams with the ACI-cut-off alternates, the beams with no cut-off, and the AASHTO beam with stirrups, this equation gives a good prediction of the diagonal cracking load. For the beams with the theoretical cut-off and the AASHTO beam without stirrups, however, the equation does not compare very favorably with the test results.

Ultimate Shear Strength

For beams without web reinforcement Committee 326 recommended that the load producing the diagonal tension crack should be considered as the ultimate load capacity in shear. This resulted in a conservative estimate for the beams with the ACI cut-off alternates and the beams with no cut-off. The predicted ultimate load for the beam with the AASHTO cut-off compared exactly. The beam with the theoretical cut-off, however, was greatly over-estimated.

For beams with stirrups Committee 326 recommended the following formula for ultimate shear strength:

$$v_u = \frac{V_u}{bd} = v_c + v_s$$

TABLE 4.

COMPARISON OF STRENGTHS WITH ACI-ASCE
COMMITTEE 326 RECOMMENDATIONS

Beam Designation	Diagonal Cracking Strength			Ultimate Shear Strength		
	v_c^* test	v_c^{**} calc.	$\frac{v_c^{\text{test}}}{v_c^{\text{calc.}}}$	v_u test	v_u^{***} calc.	$\frac{v_u^{\text{test}}}{v_u^{\text{calc.}}}$
IA	70	131	.54	98	131	.75
IB	107	143	.75	144	143	1.00
IC	158	139	1.14	172	139	1.25
ID	174	139	1.25	174	139	1.25
IE	158	143	1.10	223	143	1.56
IIA	93	139	.67	195	212*	.92
IIB	163	141	1.16	274	273	1.00
IIC	163	145	1.12	259	218*	1.23
IID	163	146	1.12	311	279	1.12
IIIA (IB)	107	143	.75	144	143	1.00
IIIB	116	143	.81	135	143	.95
IIIC	135	127	1.06	135	127	1.06
IIID	149	131	1.14	149	131	1.14

* Based upon new No. 4 Soft Wire having $f_y = 20$ ksi

$$** v_c = \frac{V_c}{bd} = 1.9 \sqrt{f'_c} + 2500 \frac{pVd}{M}$$

$$*** v_u = \frac{V_u}{bd} = v_c + Krf_{ry} \text{ for beams with stirrups}$$

$$v_u = v_c \text{ for beams without stirrups}$$

where v_s is the portion of the total unit shear assumed to be carried by the stirrups, as given by the truss analogy. Thus,

$$v_s = K \frac{A_v}{bs} f_{vy} \text{ or } K r f_{vy}$$

where $K = 1$ for vertical stirrups. Hence.

$$v_u = 1.9 \sqrt{f'_c} + 2500 \frac{pVd}{M} + K r f_{vy}$$

As shown in Table (4), the test values for Series II agreed reasonably well with the predicted values, with the exception of Beam IIA.

In Table (5) the test results are also compared with the allowable shear strengths given by the design criteria of the current "Standard Specification for Highway Bridges." These requirements provide for an allowable shearing stress (v_a) for beams without stirrups - computed by $v_c = \frac{V}{bjd}$ of $0.03f'_c$ or 90 psi maximum. For beams with vertical stirrups the allowable shearing stress is given by

$$v_a = \frac{V}{bjd} = 90 + r f_v$$

where f_v is the working stress for the stirrup steel. The value for f_v was not constant due to the use of a different strength stirrup wire in some of the beams. The allowable stirrup stress was $f_v = 18,000$ psi for the stirrup wire first used. The allowable stress was $f_v = 10,000$ psi for the new stirrup wire.

For beams without web reinforcement (Series I) the beams with the ACI cut-off alternates (IC and ID) and the beam with no cut-off (IE) showed a factor of safety greater than 2.0. However, the beam with AASHTO cut-off (IB) had a factor of safety of only 1.83, whereas the beam with the theoretical cut-off (IA) had a factor of safety of only 1.24.

For beams with reinforcement (Series II) the beams with the AASHO, ACI, and no cut-off all had a factor of safety of more than 2.0. Only the beam with the theoretical cut-off (IIA) had a lower factor of safety 1.77.

For beams with the compressive strength as a variable (Series III) and the AASHO cut-off as a constant, the factor of safety was less than 2.0 in each case. However, it was found that a sudden type of diagonal tension failure occurred in the beams of lower strength and hence, with respect to shear, they had the same ultimate load capacity.

TABLE 5.

COMPARISON OF STRENGTHS WITH AASHO
 "STANDARD SPECIFICATIONS FOR HIGHWAY BRIDGES"

Beam Designation	v_u^{**} test (psi)	rf_v (psi)	v_a (psi)	$\frac{v_u}{v_a}$
IA	112	...	90	1.24
IB	165	...	90	1.83
IC	197	...	90	2.19
ID	199	...	90	2.21
IE	255	...	90	2.83
IIA	223	36*	126	1.77
IIB	313	65	155	2.02
IIC	308	36*	126	2.44
IID	356	65	155	2.30
IIIA (IB)	165	...	90	1.83
IIIB	154	...	90	1.71
IIIC	154	...	90	1.71
IIID	170	...	90	1.89

* Based upon new No. 4 Soft Wire having $f_y = 20$ ksi

** v_u test = $\frac{Vu}{bjd}$ or practically $\frac{8Vu}{7bd}$

* $v_a = 90$ psi for beams without stirrups

$v_a = 90 + rf_v$ for beams with stirrups

SUMMARY AND CONCLUSIONS

1. The diagonal cracking strength of beams without web reinforcement as compared to the Committee 326 recommendations was directly related to the point of bar cut-off. In addition, the beam with no cut-off as compared to the ACI alternatives had no additional cracking strength, and only slight additional ultimate shear strength, thus confirming the ACI cut-off alternatives as valid methods for bar cut-off. The AASHTO cut-off, however, was definitely not within reasonable proximity of the recommendations of the Committee 326.

2. The diagonal cracking strength and the ultimate shear strength of the beams with web reinforcement (with the exception of beam IIA) compared favorably with the recommendations of the Committee. This indicated that the influence of the location of bar cut-off on beam behavior was effectively diminished due to the web reinforcement. Hence, the cut-off location was not as critical in this case.

3. The ultimate shear strength of beams without web reinforcement as compared to the AASHTO allowable shear strength was similarly related to the point of bar cut-off (Table 5). The ACI alternatives (IC and ID) and the beam with no cut-off (IE) had a factor of safety above 2.0. In fact, IE had a factor of safety of 2.83, which indicated that the additional steel made the design of the beam much more conservative than would be consistent with the other design procedures and factors of safety. The beam with AASHTO cut-off (IB), however, had a factor of safety of only 1.83, indicating that the present AASHTO Specifications are unconservative with respect to bar cut-off in tension reinforcement.

4. The ultimate shear strength of beams with web reinforcement as compared to the AASHTO allowable shear strength indicated that the influence of the location of bar cut-off on beam behavior was effectively diminished due to the web reinforcement, as was previously mentioned in Conclusion 2.

5. The effect of bar cut-off upon unsymmetrical bending, although it did not develop until near the failure load, was apparent. The extent to which it developed was definitely associated with the location of the bar cut-off. Again, the use of stirrups diminished this effect.

6. The use of stirrups around the AASHTO cut-off point (ID) increased substantially the diagonal cracking strength and the ultimate shear strength capacity of the beam and provided a higher, more conservative factor of safety.

SUGGESTIONS FOR FURTHER RESEARCH

1. The beams of this study held the shear span to depth ratio constant. In subsequent studies the effect of this ratio coupled with the location of bar cut-off upon the shear strength of beams could be investigated.

2. The two different types of diagonal tension failure - sudden vs. slowly propagating - and their effects upon ultimate shear strength which were experienced in Series III with concrete strength as a variable indicate that further research is needed to determine the correlation between these variables.

BIBLIOGRAPHY

1. ACI-ASCE Committee 326, "Shear and Diagonal Tension," ACI Journal, Jan., Feb. 1962 Proceedings, Vol. 59.
2. ACI Committee 318, "Building Code Requirements for Reinforced Concrete (ACI 318-63)," ACI Standard, June, 1963.
3. American Association of State Highway Officials (AASHO), "Standard Specifications for Highway Bridges," 1961.
4. Harvey, W. N., "A Study of Diagonal Tension Failure in Reinforced Concrete Beams," Joint Highway Research Project, Purdue University, Lafayette, Indiana, Sept. 1964, No. 24.

APPENDIX

Sample Calculations

For All Beams:

$$p_w = \frac{A_s}{bd} = \frac{2(.44)}{(6)(11.10)} = 0.0132$$

The critical point for shear is at a distance d from the support. At this point

$$\frac{V}{M} = \frac{1}{a-d}$$

UNREINFORCED WEB: Beam 1B

$$f_c' = 4380 \text{ psi}$$

AASHTO Allowable Shear Stress:

$$v_a = \frac{V}{bjd} = 0.03f_c' = 0.03(4380) = 132 \text{ psi}$$

However, the maximum shear stress permitted is 90 psi and hence,

$$v_a = 90 \text{ psi}$$

ACI Allowable Shear Stress:

Using the Committee 326 recommendations (ACI Equation 12-2)

$$v_c = \frac{V}{bd} = \sqrt{f_c'} + 1300 \frac{p_w Vd}{M}$$

thus

$$v_c = \sqrt{4380} + 1300 \frac{(.0132)(11.10)}{(32 - 11.10)}$$

or

$$= 66 + 9$$

or

$$v_c = 75 \text{ psi}$$

ACI Ultimate Shear Stress:

The Committee recommendation for ultimate shear stress which is equivalent to the diagonal cracking strength for an unreinforced web is 1.9 times the allowable shear stress (ACI Equation 17-2).

Thus,

$$v_u = 1.9 v_o = 1.9 (75) = 143 \text{ psi}$$

REINFORCED WEB: Beam IIB

$$f'_c = 4210 \text{ psi}$$

For beams with web reinforcement, the web reinforcement ratio is also required:

$$r = \frac{A_v}{bs} = \frac{(2)(.0380)}{(6)(3.5)} = .00362$$

AASHTO Allowable Shear Stress:

$$v_a = \frac{V}{b_j d} = 0.03 f'_c + f_v$$

where

$$f_v = 18,000 \text{ psi}$$

for the stirrup steel used

Thus,

$$v_a = 90 + (.00362)(18,000)$$

$$\text{or} \quad = 90 + 65$$

$$\text{or} \quad v_a = 155 \text{ psi}$$

ACI Diagonal Cracking Strength

The Committee recommendation (ACI Equation 17-2) is

$$v_c = \frac{V}{bd} = 1.9 \sqrt{f'_c} + 2500 \frac{p_v V_d}{M}$$

or

$$v_c = 1.9 \sqrt{4210} + 2500 \frac{(.0132)(11.10)}{(32 - 11.10)}$$

or

$$v_c = 123 + 18$$

or

$$v_c = 141 \text{ psi}$$

ACI Ultimate Shear Strength

$$v_u = v_c + rf_{vy}$$

where

$$f_{vy} = 36,600 \text{ psi}$$

for the stirrup steel used.

Hence,

$$v_u = 141 + (.00362)(36.6)$$

or

$$v_u = 141 + 132$$

or

$$v_u = 273 \text{ psi}$$